

THE SUDETIC MARGINAL FAULT: A YOUNG MORPHOTECTONIC FEATURE OF CENTRAL EUROPE

Janusz BADURA ¹, Witold ZUCHIEWICZ ²,
Petra ŠTĚPANČIKOVÁ ³,
Bogusław PRZYBYLSKI ¹, Bernard KONTNY ⁴ &
Stefan CACOŃ ⁴

¹ Lower Silesian Branch, Polish Geological Institute, Al. Jaworowa 19, 50-122 Wrocław, Poland; e-mails: janusz.badura@pgi.gov.pl, boguslaw.przybylski@pgi.gov.pl

² Institute of Geological Sciences, Jagiellonian University, ul. Oleandry 2A, 30-063 Kraków, Poland; e-mail: witold@ing.uj.edu.pl

³ Institute of Rock Structure and Mechanics, Academy of Sciences of the Czech Republic, V Holešovičkách 41, 182 09 Prague, Czech Republic; e-mail: petstep@centrum.cz

⁴ Institute of Geodesy and Geoinformatics, Wrocław University of Environmental and Life Sciences, ul. Grunwaldzka 53, 50-357 Wrocław, Poland; e-mails: kontny@kgf.ar.wroc.pl, cacon@kgf.ar.wroc.pl

OUTLINE

INTRODUCTION

GEOLOGICAL SETTING

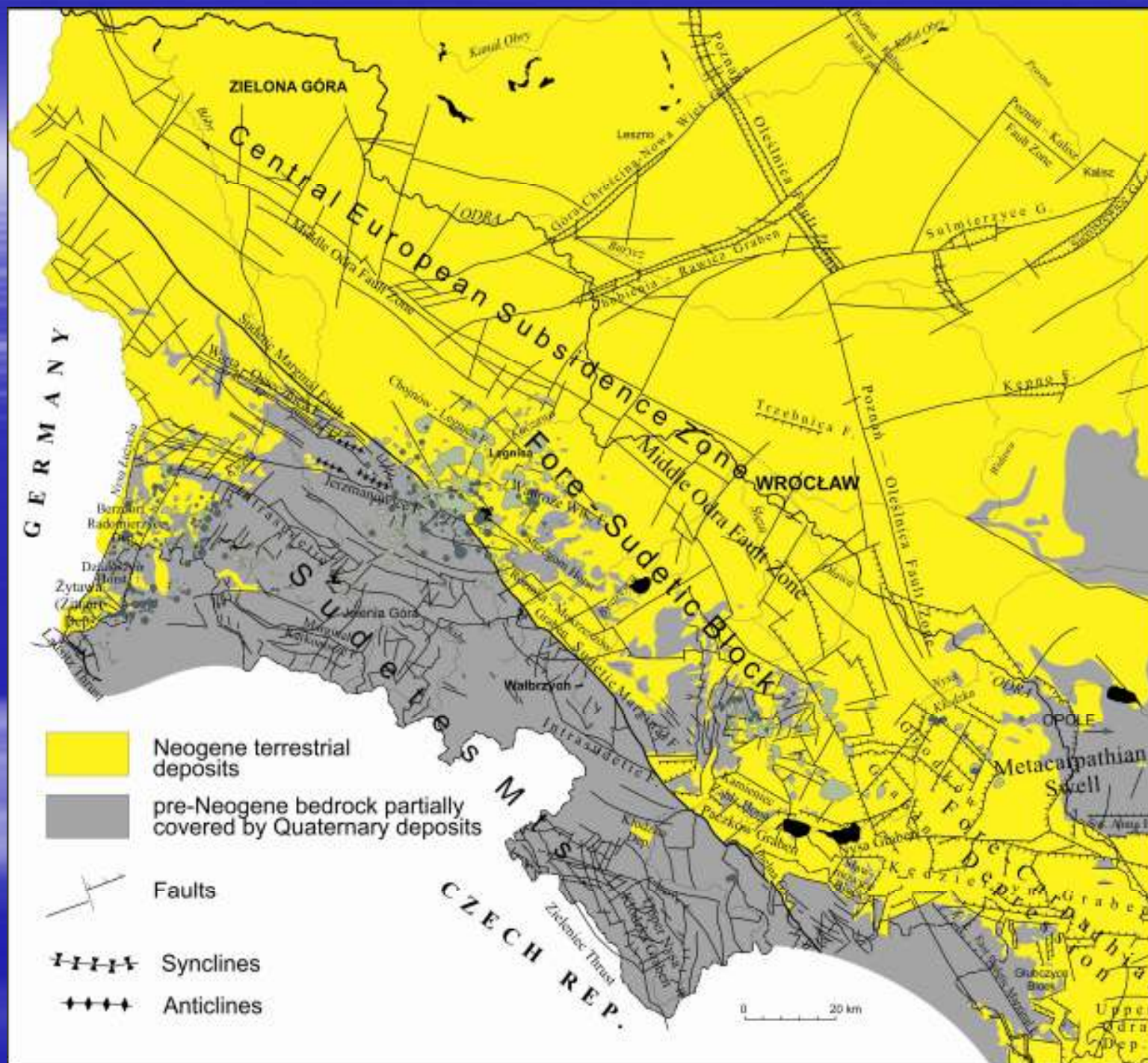
METHODS

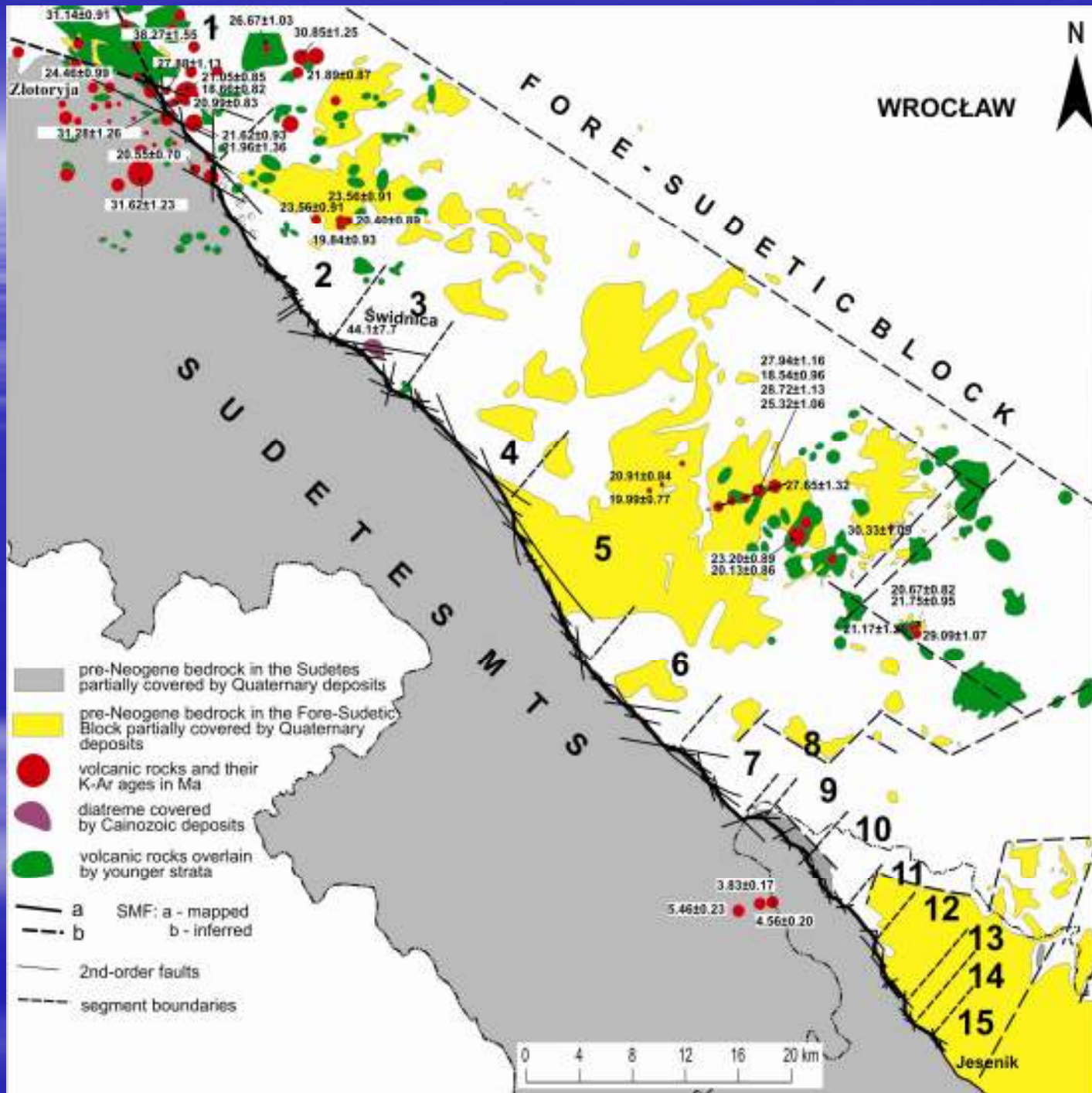
TIERING OF FACETED SPURS

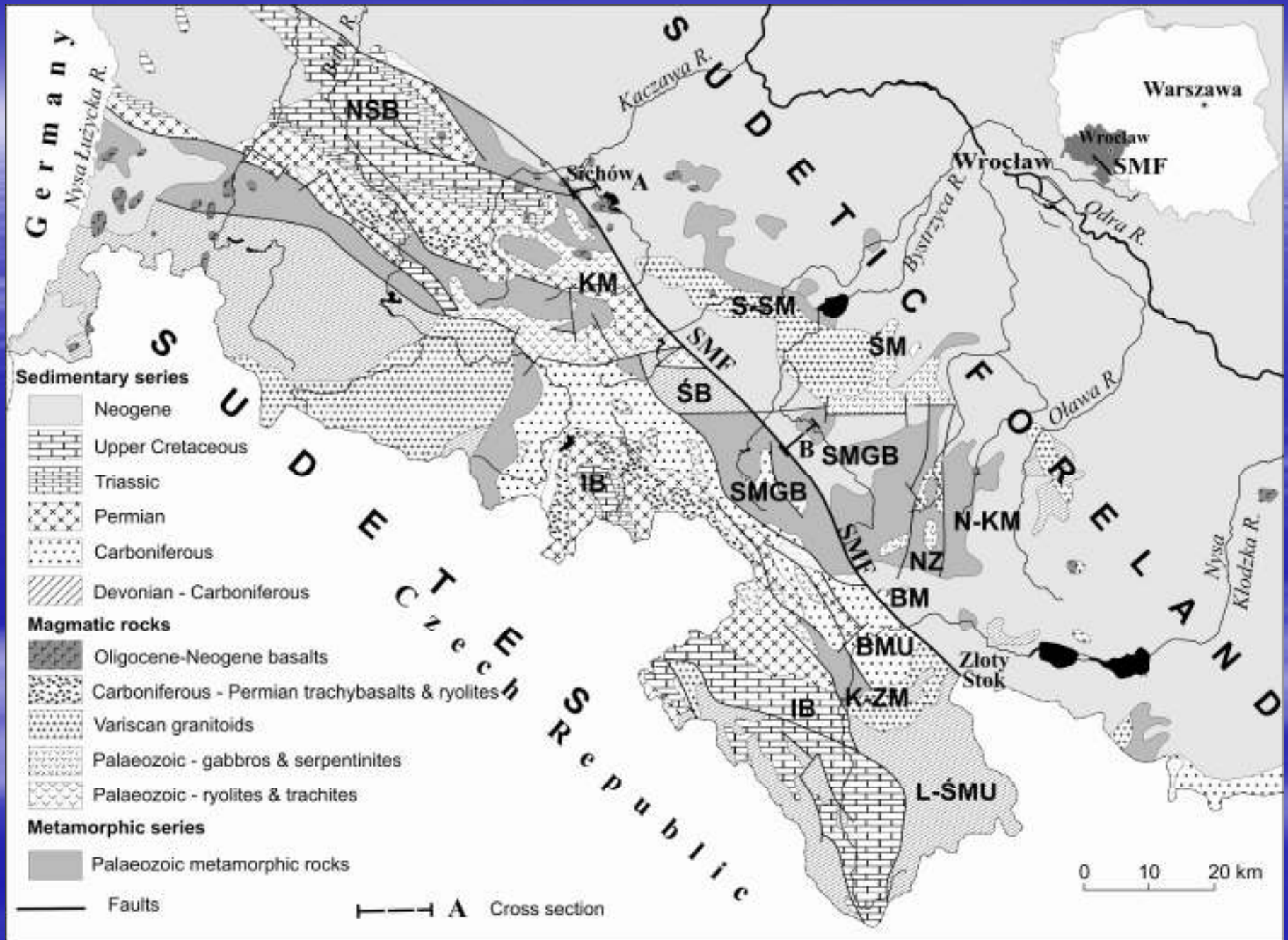
SMALL-SCALE DRAINAGE BASINS

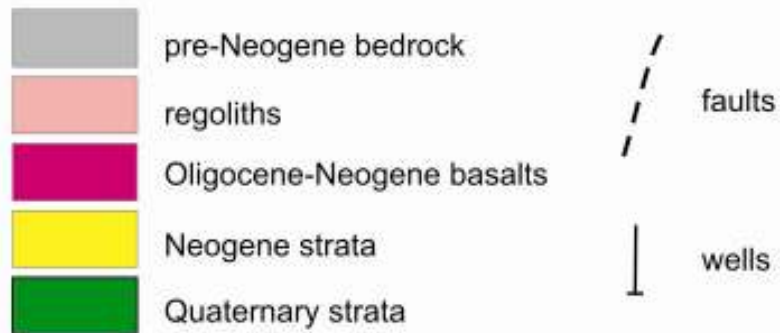
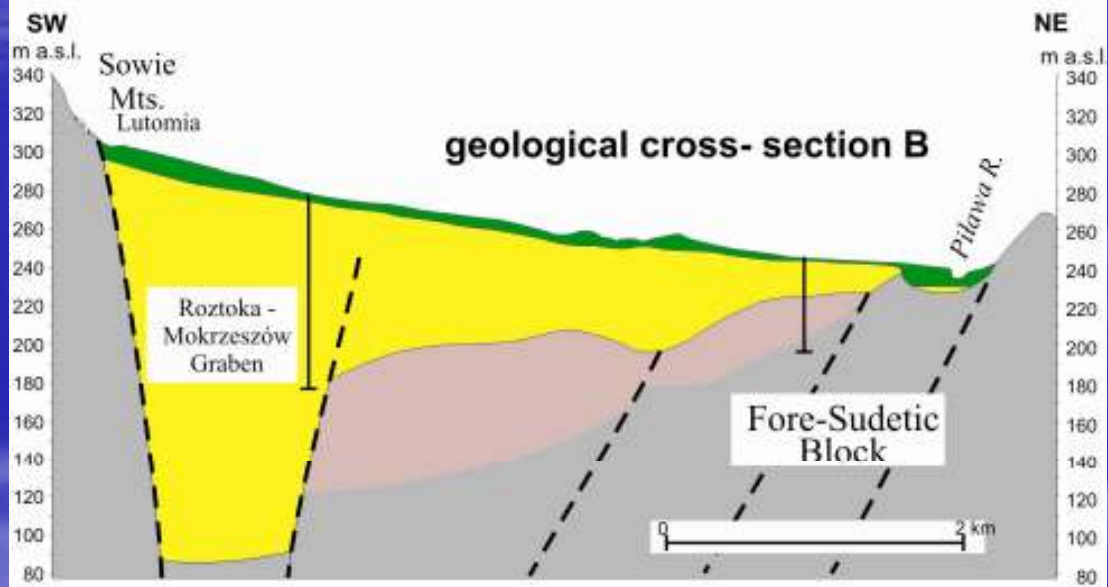
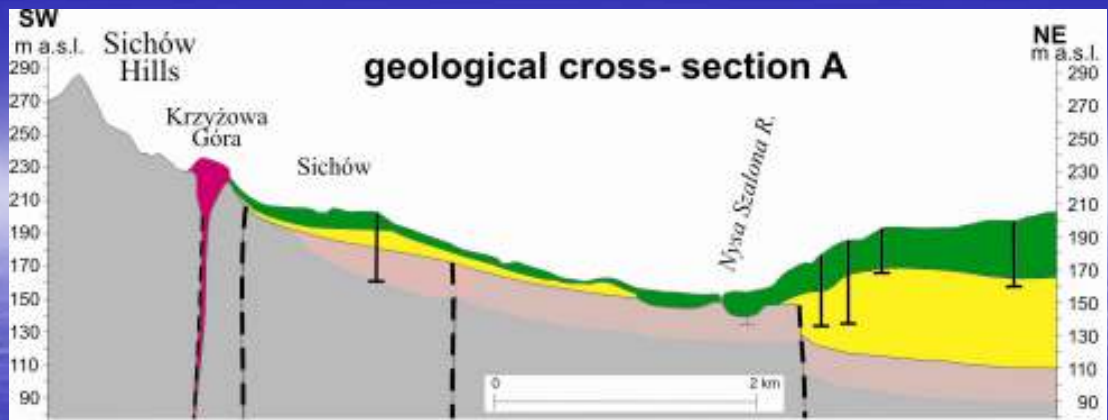
GEODETTIC CONSTRAINTS

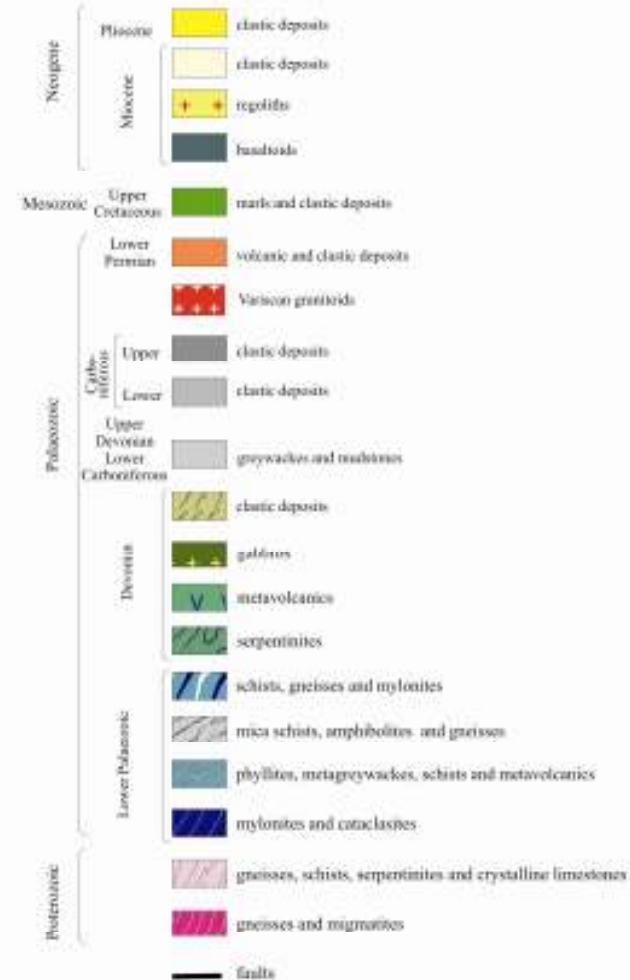
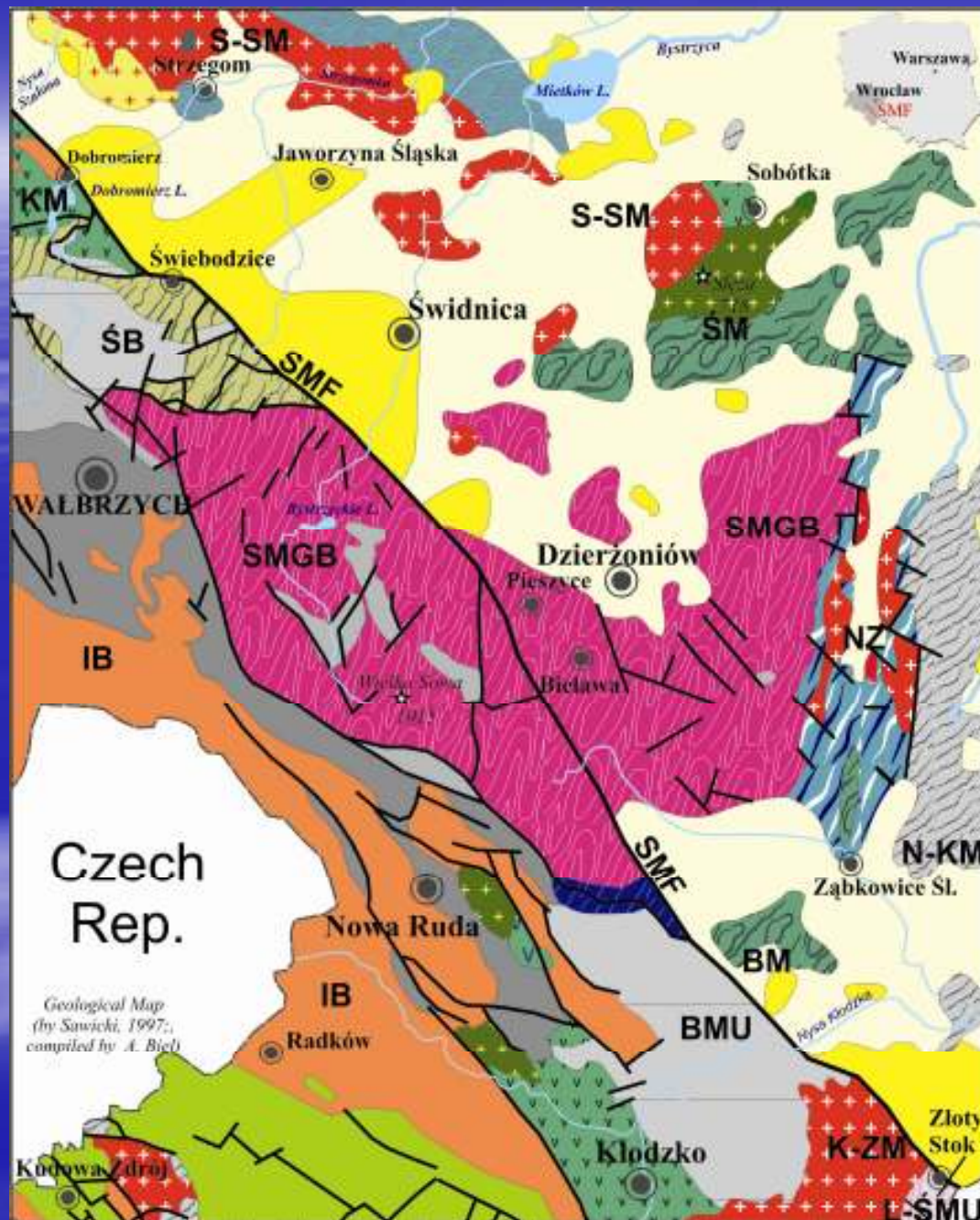
CONCLUSIONS







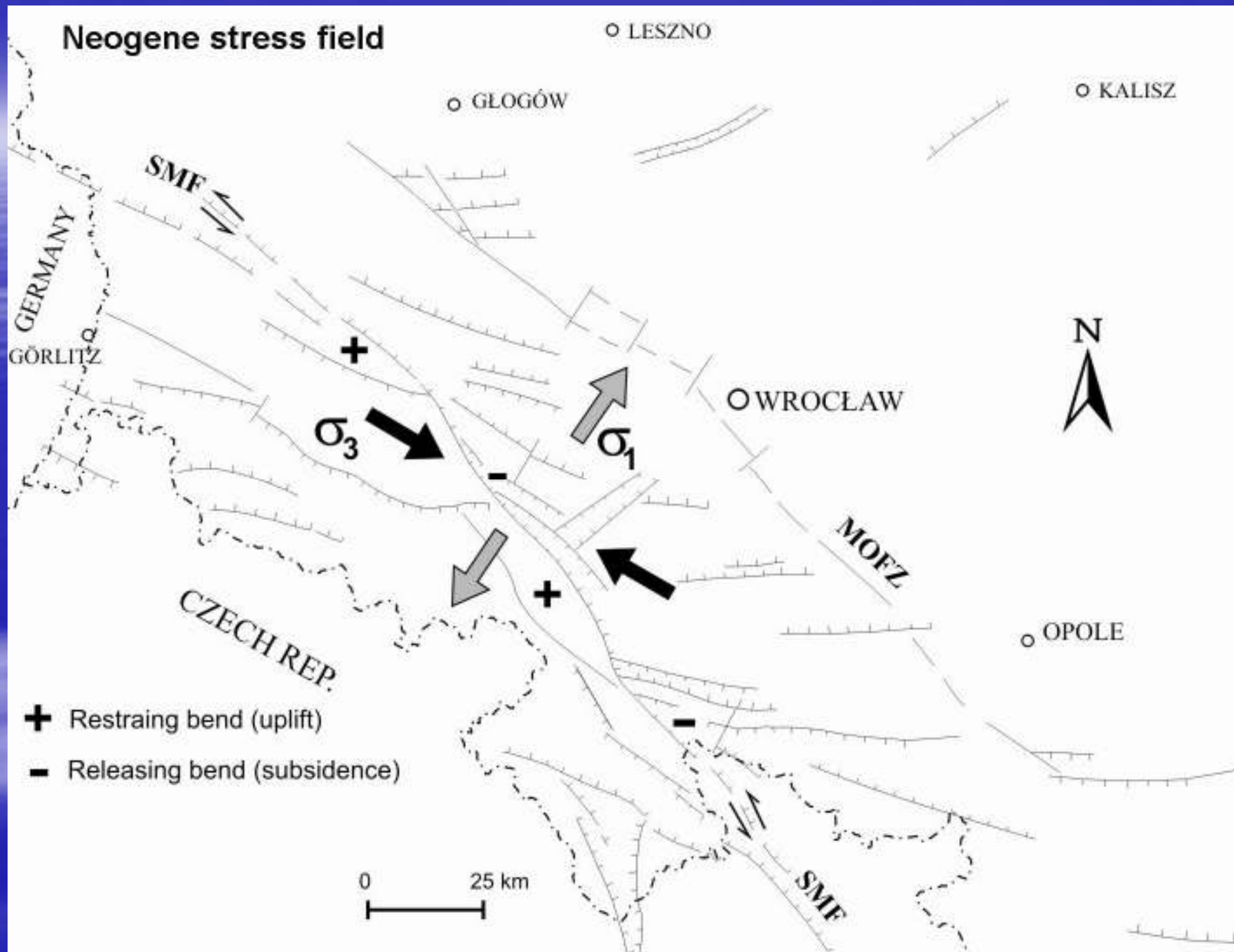


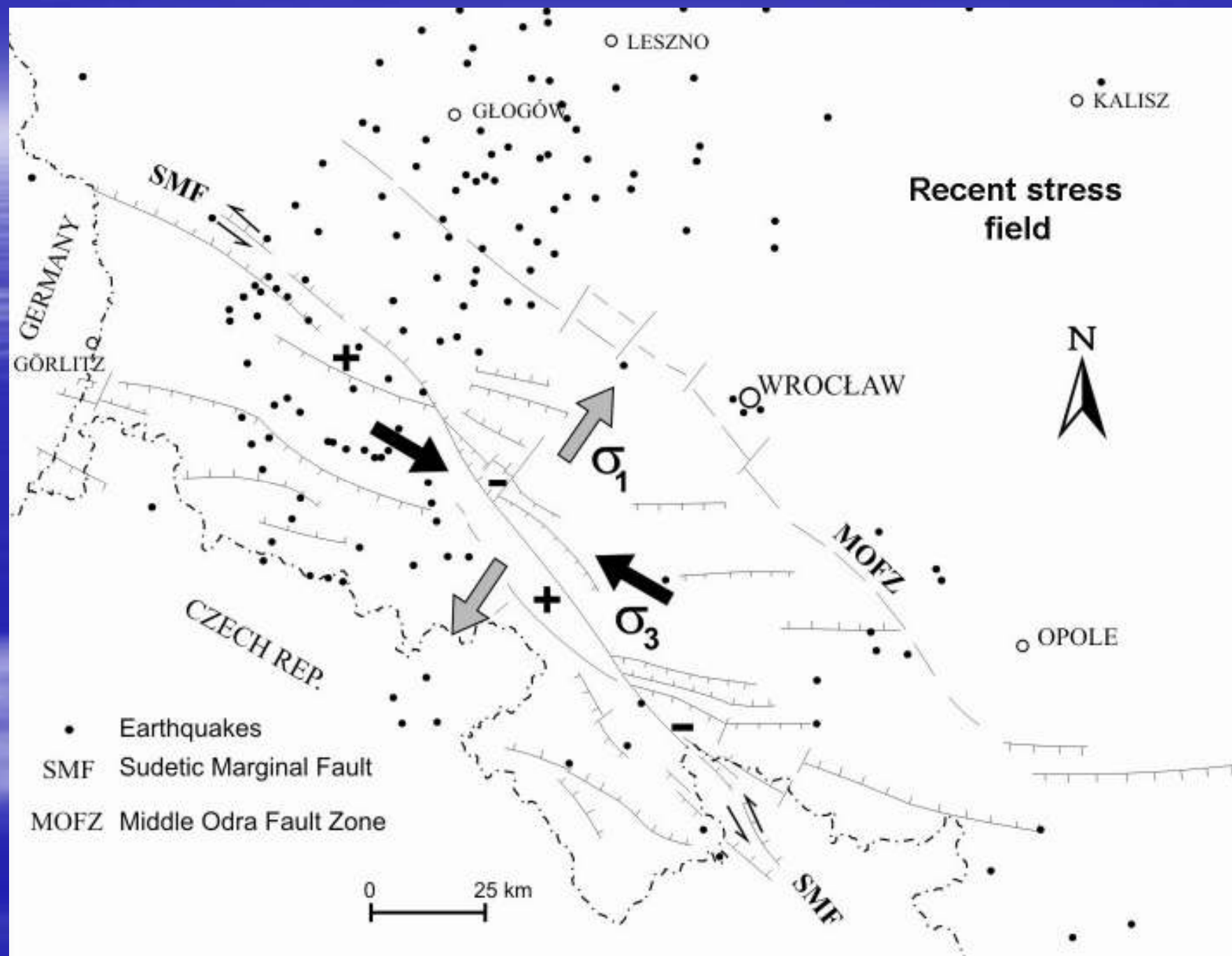


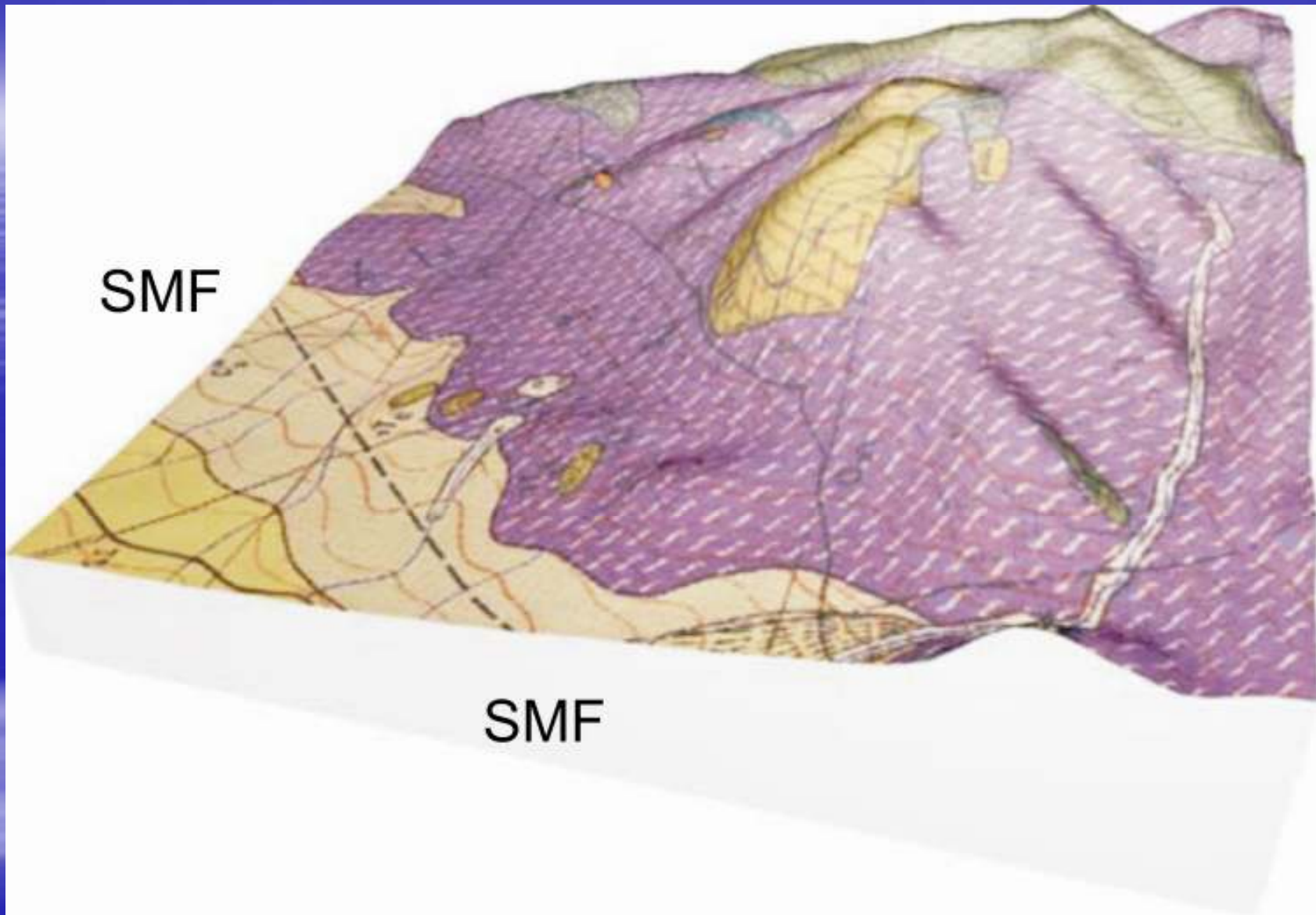
BM - Brzeźnica Massif, BMU - Bardo Mts Unit, IB - Intrasudetic Basin, K-ZM - Kłodzko-Złoty Stok Massif, L-ŚMU - Łądek-Śnieżnik Metamorphic Unit, N-KM - Niemcza-Kamieniec Metamorphic, NZ - Niemcza Zone, SMGB - Sowie Mts gneissic block, S-SM - Strzegom-Sobótka Massif, ŚB - Świebodzice Basin, ŚM - Śleza Massif; SMF - Sudetic Marginal Fault

0 3 6 9 12 15 km

Neogene stress field



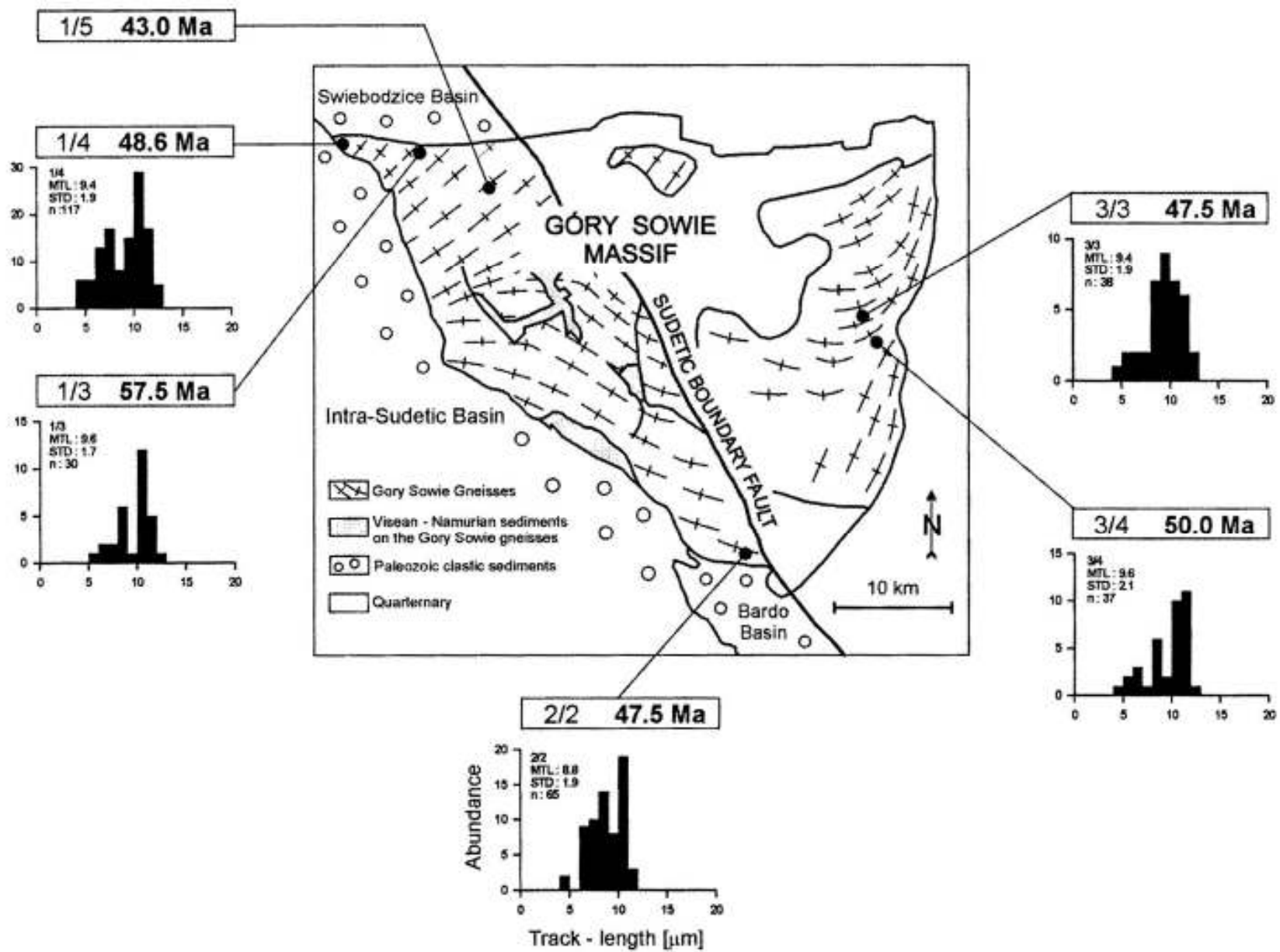




basalts at Değbina



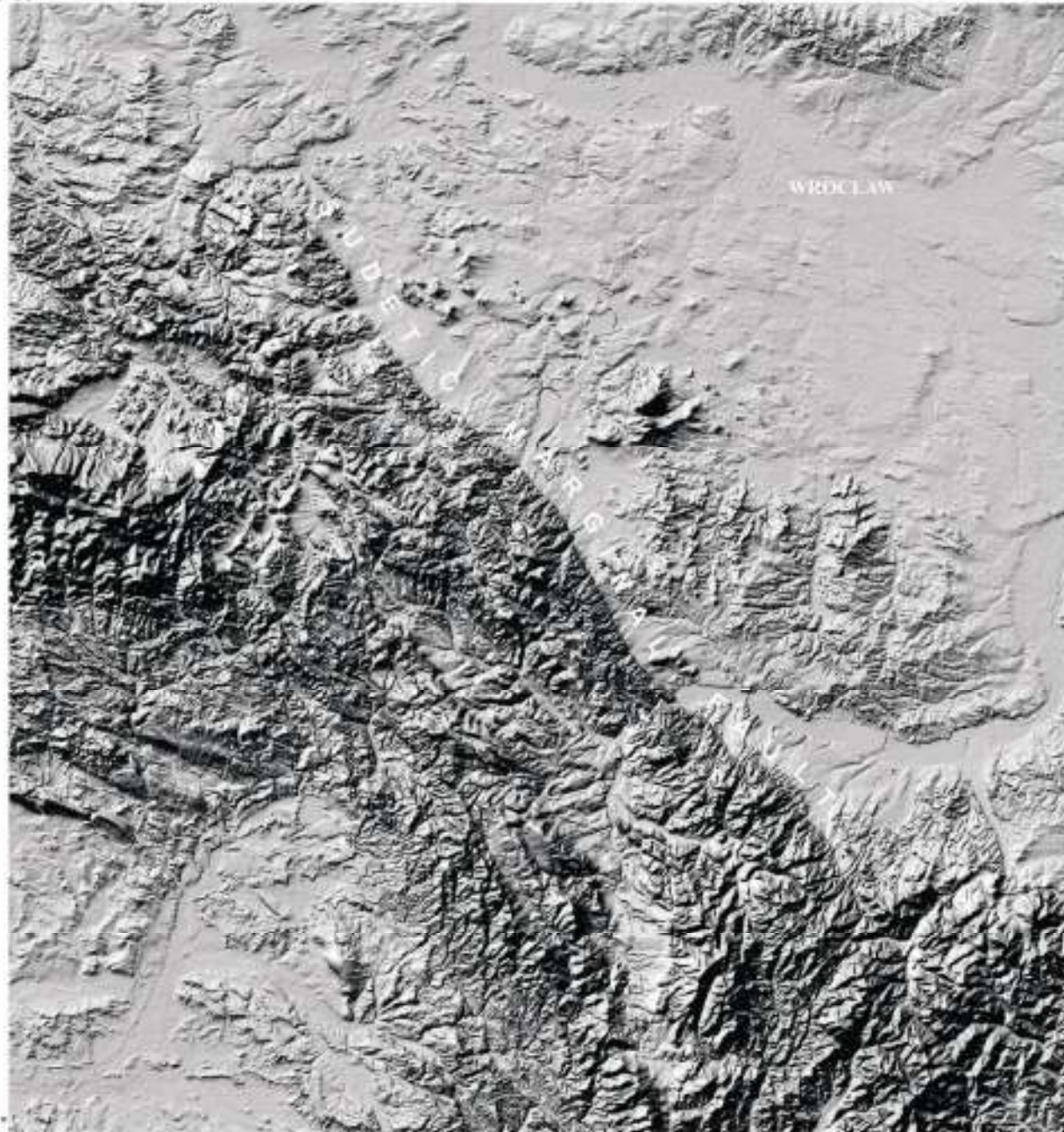
Outline geology of the Sudetes (after Aramowicz et al., 2006)



**Góry Sowie Massif and the results of apatite fission-track dating
(after Aramowicz et al., 2006)**

15°30'

51°
20'



WROCLAW

51°
20'

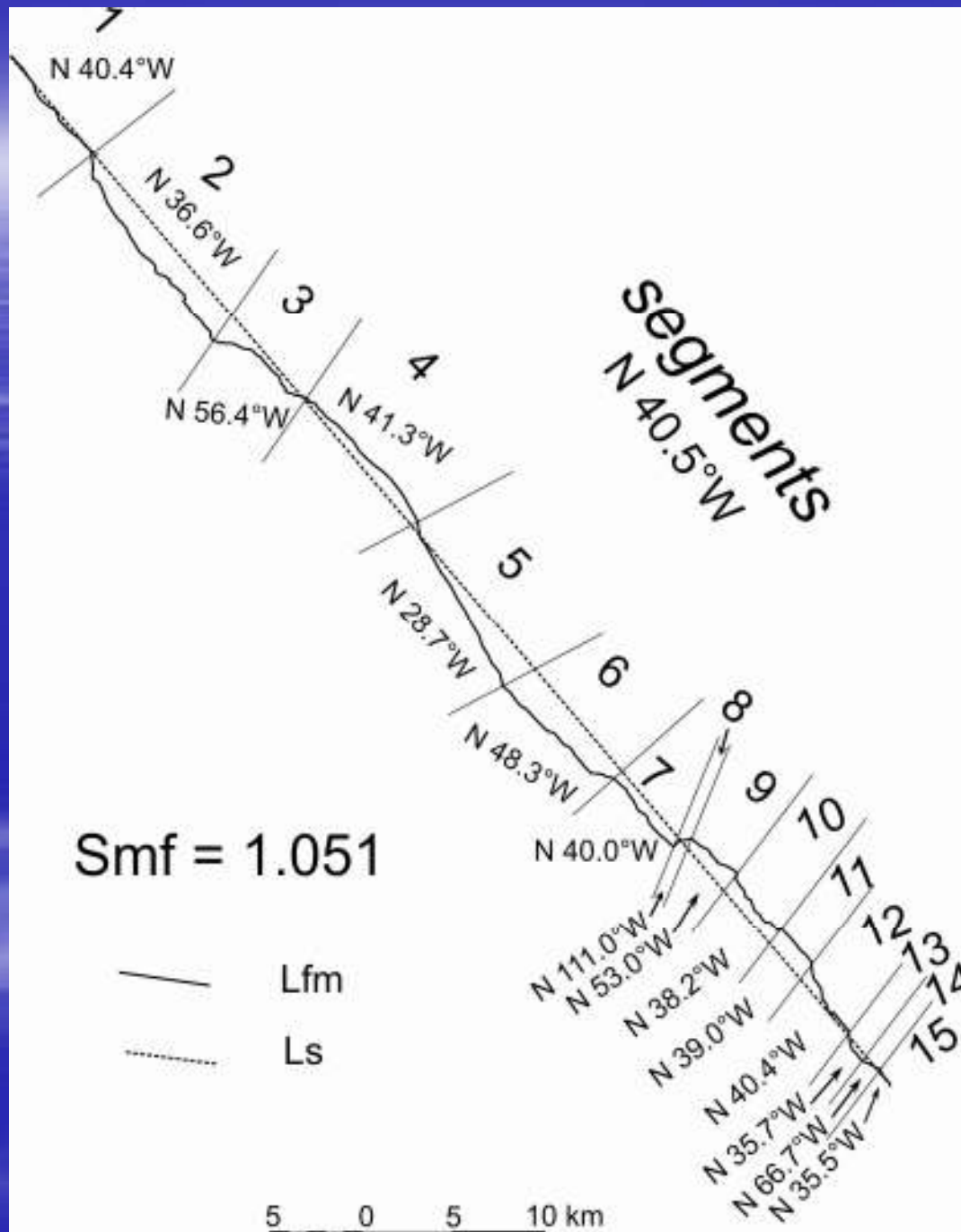
0 25 km

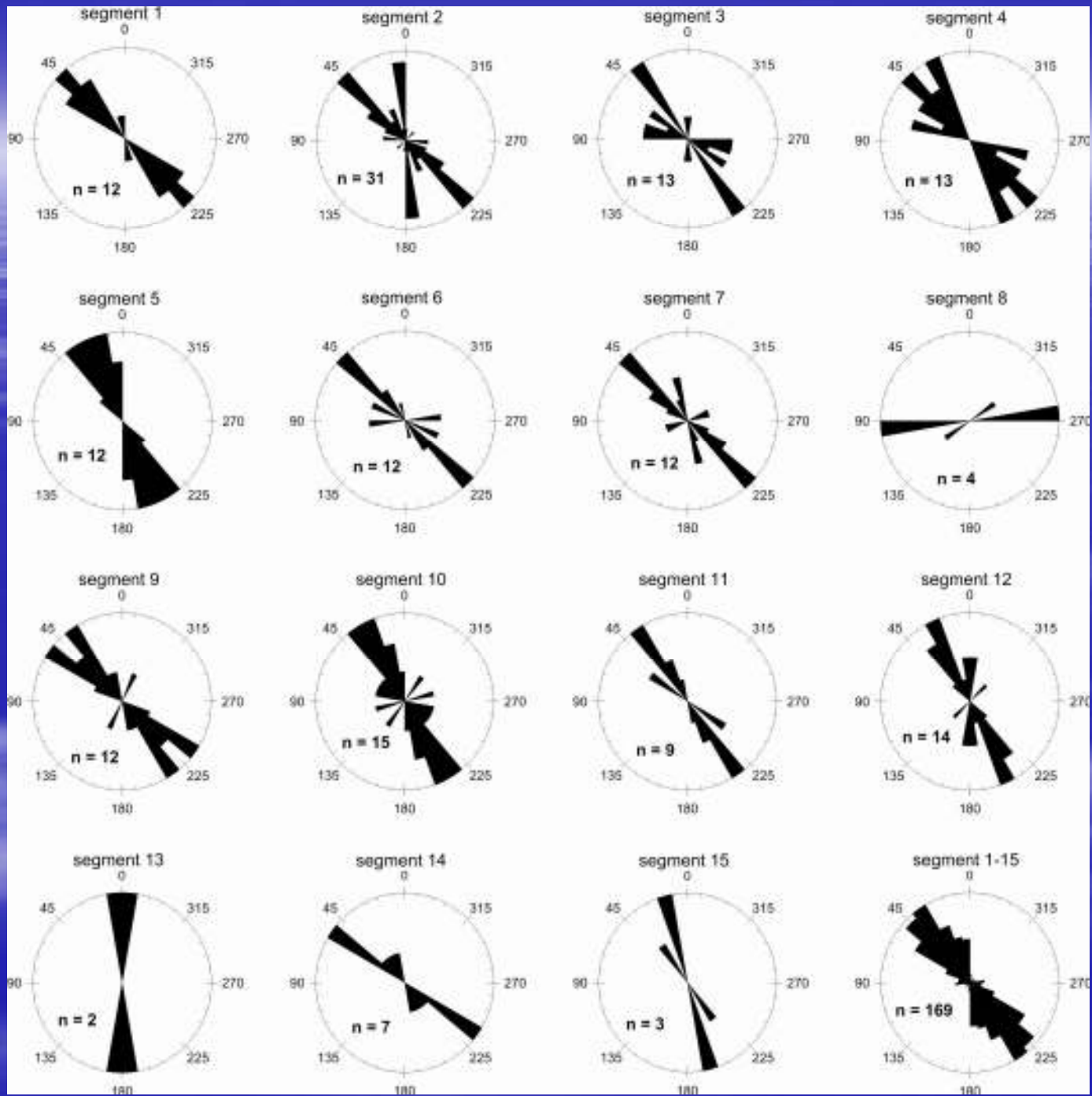
17°30'

We analysed a nearly 140-km-long portion of the Sudetic Marginal Fault (SMF) in Poland (99.7 km) and the Czech Republic (37.4 km), comprised between Złotoryja in the NW and Jeseník in the SE.

The fault trace has been subdivided into fifteen segments showing different orientation (N29°W to N56°W, and even N111°W SE of Złoty Stok), geological setting, length (8.8-22.9 km in Poland and 1.4-7.8 km in the Czech Republic), and height of the fault and fault-line scarps (5-75 m to 200-360 m).

At the foot of the mountain front cut by the SMF, two large (Dobromierz, Javorník) and two minor (Sichów, Świebodzice) fault steps occur. Orientation of the entire fault trace approaches N41°W, and the mountain front sinuosity amounts to 1.051.

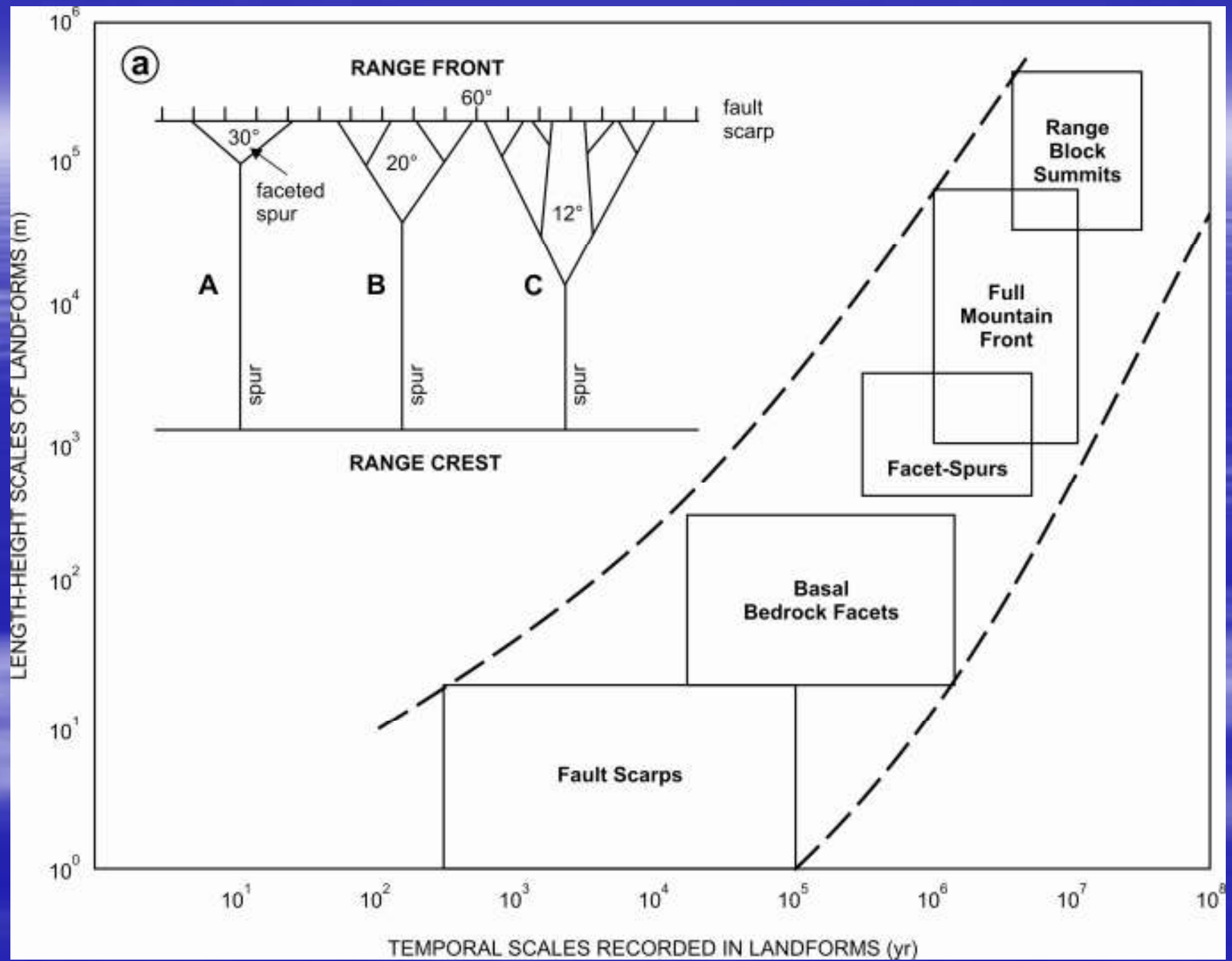




Active *fault-generated mountain fronts* are either straight (normal faulting) or sinuous and embayed (thrusting), and frequently display *triangular or trapezoidal facets (faceted spurs, flatirons)* that form due to uplift and dissection of a normal scarp by gullies and whose bases are parallel to the fault trace (Cotton, 1950; Bloom, 1978; Stewart & Hancock, 1990).

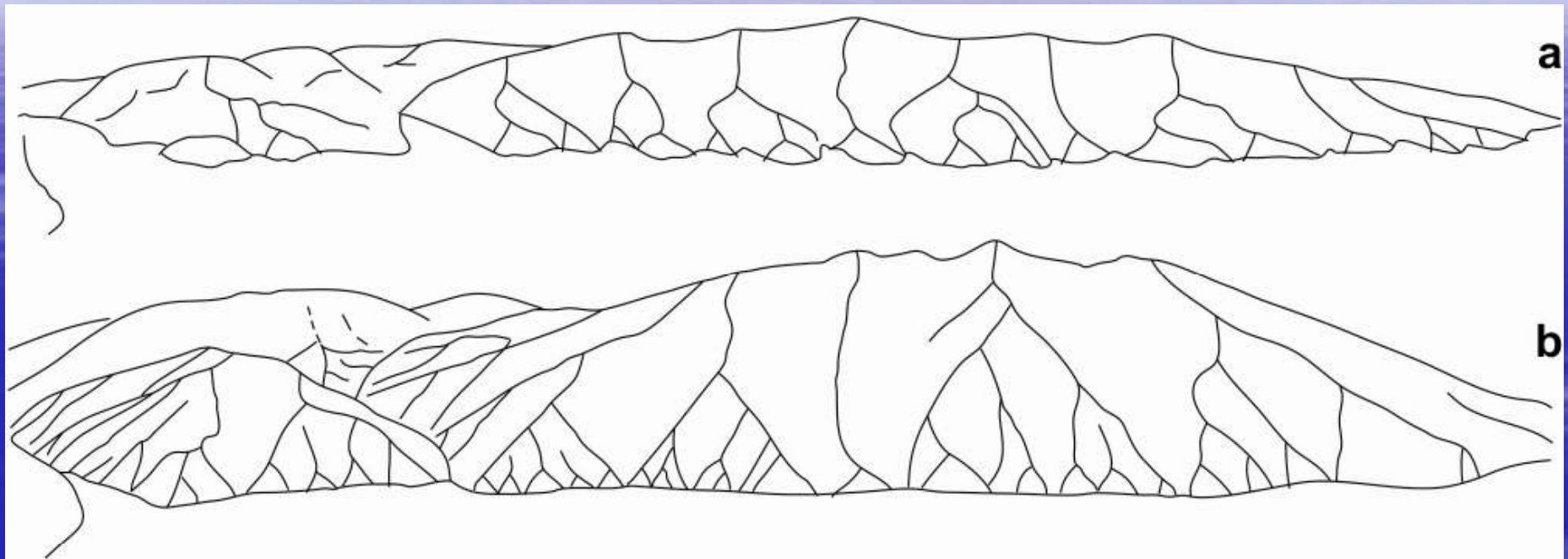
The triangular facet occurs only where the spur is sharp-crested. If the spur were flat-topped, the facet would be trapezoidal. The slope of the facets range 25-35°, whereas the fault plane dips at 50-90° (Wallace, 1978). The spacing of facets along range fronts depends on the evolution of drainage basins within the footwall block.

Flights of faceted spurs have been interpreted as a result of either episodic uplift (Hamblin, 1976; Anderson, 1977), or distributed faulting within the range-bounding fault (Menges, 1988; Zuchiewicz & McCalpin, 2000). Some authors claim that facets with uniform slopes are active geomorphic features resulting from landsliding (Ellis *et al.*, 1999).



The shaping of faceted spurs is thought to result mostly from fluvial erosion concurrent with uplift of the mountain front (Hamblin, 1976; Wallace, 1978) or from gradual backwearing, aided by gravitational mass movements (*cf.* Anderson, 1977). Some authors point to the importance of subsidiary faults and fracture zones that run parallel to the main range front fault in modelling fault scarps (*cf.* Stewart & Hancock, 1988, 1990).

The size of a faceted spur is a function of the distance between major canyons incised into the mountain front and of the spur's height. The steepness of canyon walls exerts control upon main apical angles of faceted spurs. One would expect that on relatively homogeneous bedrock these angles would tend to decrease with facet's age. Departures from this trend imply lithologic control. The height of faceted spurs, in turn, is a function of uplift, whereas average inclination may be controlled by a variety of factors. One of them is the age of the spur: on homogeneous bedrock (*cf.* Wallace, 1977, 1978) the younger facets are steepest.



**Spanish Fork segment of the Wasatch fault (Anderson, 1977):
a - Palaeogene and Neogene planation, b - present**

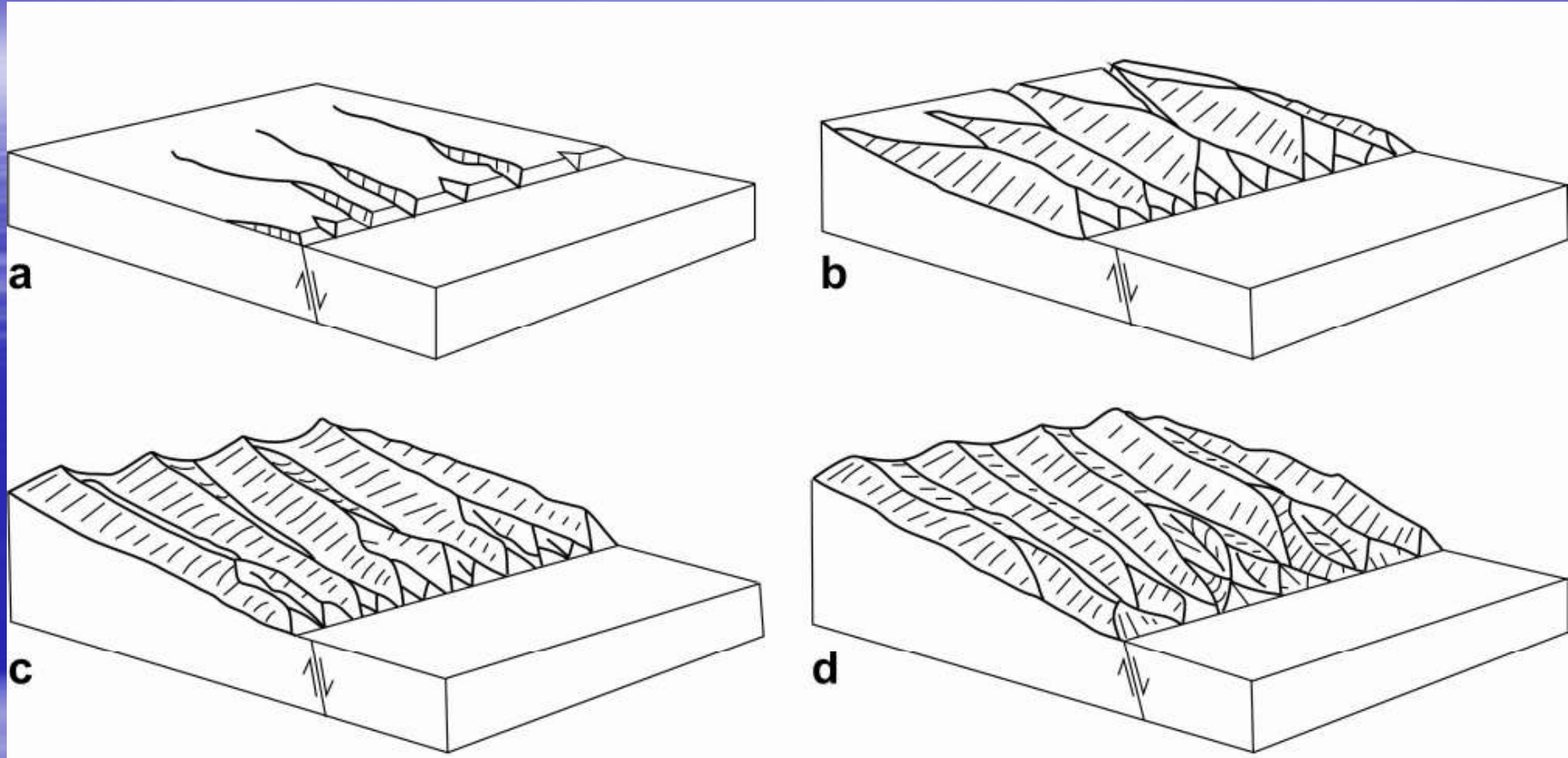


Bloom (1978)

Triangular facets aligned on the fault scarp of Maple Mountain,
15 km south of Provo, Utah. View east. (Photo: H. J. Bissell.)

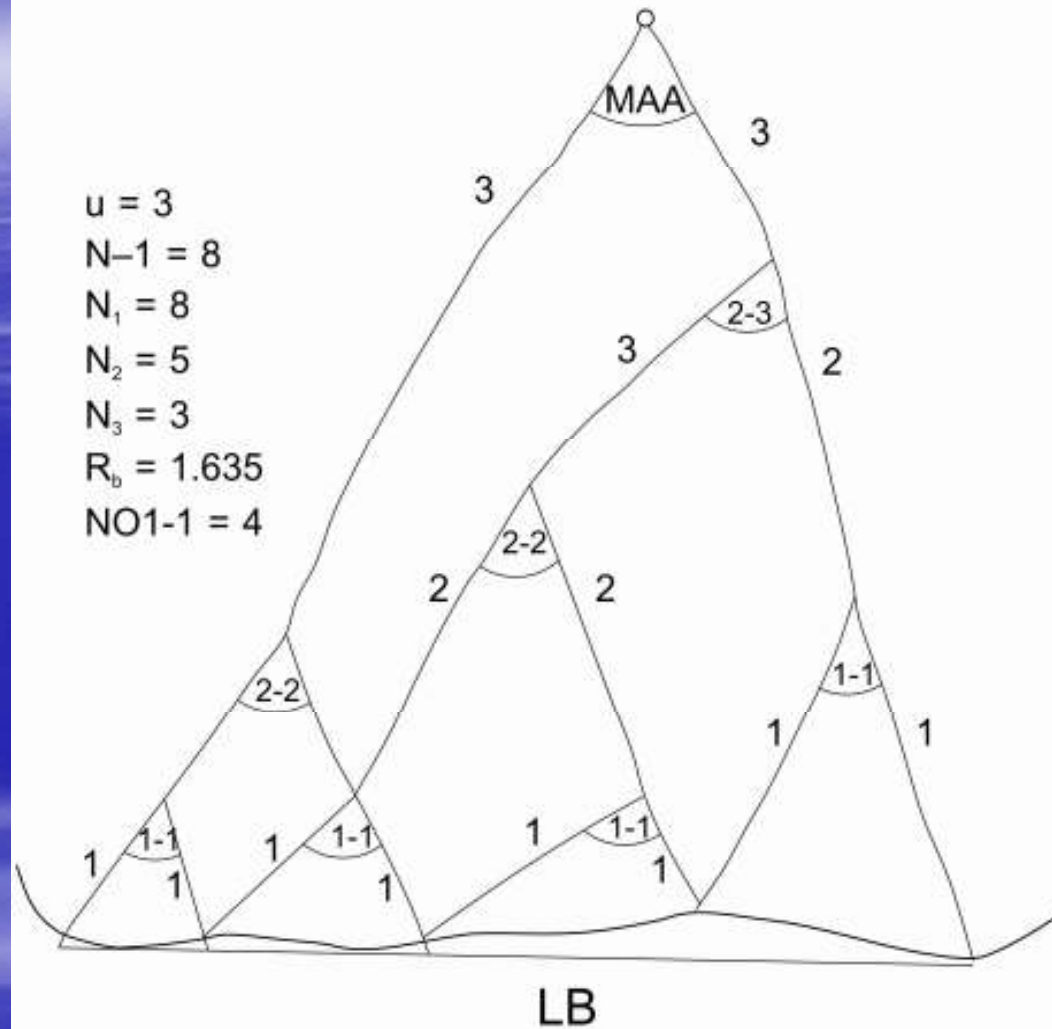
Provo, Utah





Development of compound faceted spurs (based on Anderson, 1977)

EXAMPLE OF A COMPOUND FACETED SPUR



u - link order; **N-1** - number of 1st-order links; **1-1, 2-2** - angles comprised between links of different orders; **R_b** - bifurcation ratio; **No 1-1** - number of angles comprised between 1st-order links; **MAA** - main apical angle; **LB** - the length of spur's base measured along straight line

**Parameters describing small catchment areas along
the Sudetic Marginal Fault**

Parameter	Symbol	Formula	References
total area	A		Horton (1945)
area of the basin to the right (facing downstream) of the trunk stream	AR		
asymmetry factor	Af	100(AR/A)	Hare and Gardner (1985)
maximum basin length	L		Horton (1945), Schumm (1954)
basin perimeter	P		Smith (1950)
mean width of the basin	W	A/L	
maximum relief	H	Hmax-Hmin	Strahler (1954), Schumm (1954)
basin elongation ratio	Re	2(A/π)^{0.5}/L	Schumm (1956)
form ratio	Rf	A/L²	Horton (1945)
circulatory ratio	Rk	(4πA)/P²	Miller (1953), Gregory and Walling (1973)
relief ratio	Rh	H/L	Schumm (1954, 1956)
relative relief	Rhp	H/P	Melton (1957, 1958)

BASIN ELONGATION RATIO (Bull & McFadden, 1977)

$$Re = 2(A/\pi)^{0.5}/L$$

A = drainage basin area

L = maximum basin length (distance between the two most distant points in the drainage basin)

classes of tectonic activity	Re
active	< 0.50
slightly active	0.50 - 0.75
inactive	> 0.75

VALLEY FLOOR WIDTH - VALLEY HEIGHT RATIO (Bull & Mc Fadden, 1977)

$$V_f = 2V_{fw} / [(E_{ld} - E_{sc}) + (E_{rd} - E_{sc})]$$

V_{fw} = the width of the valley floor

E_{ld} , E_{rd} , E_{sc} = the altitudes of the left and right divides and the stream, respectively

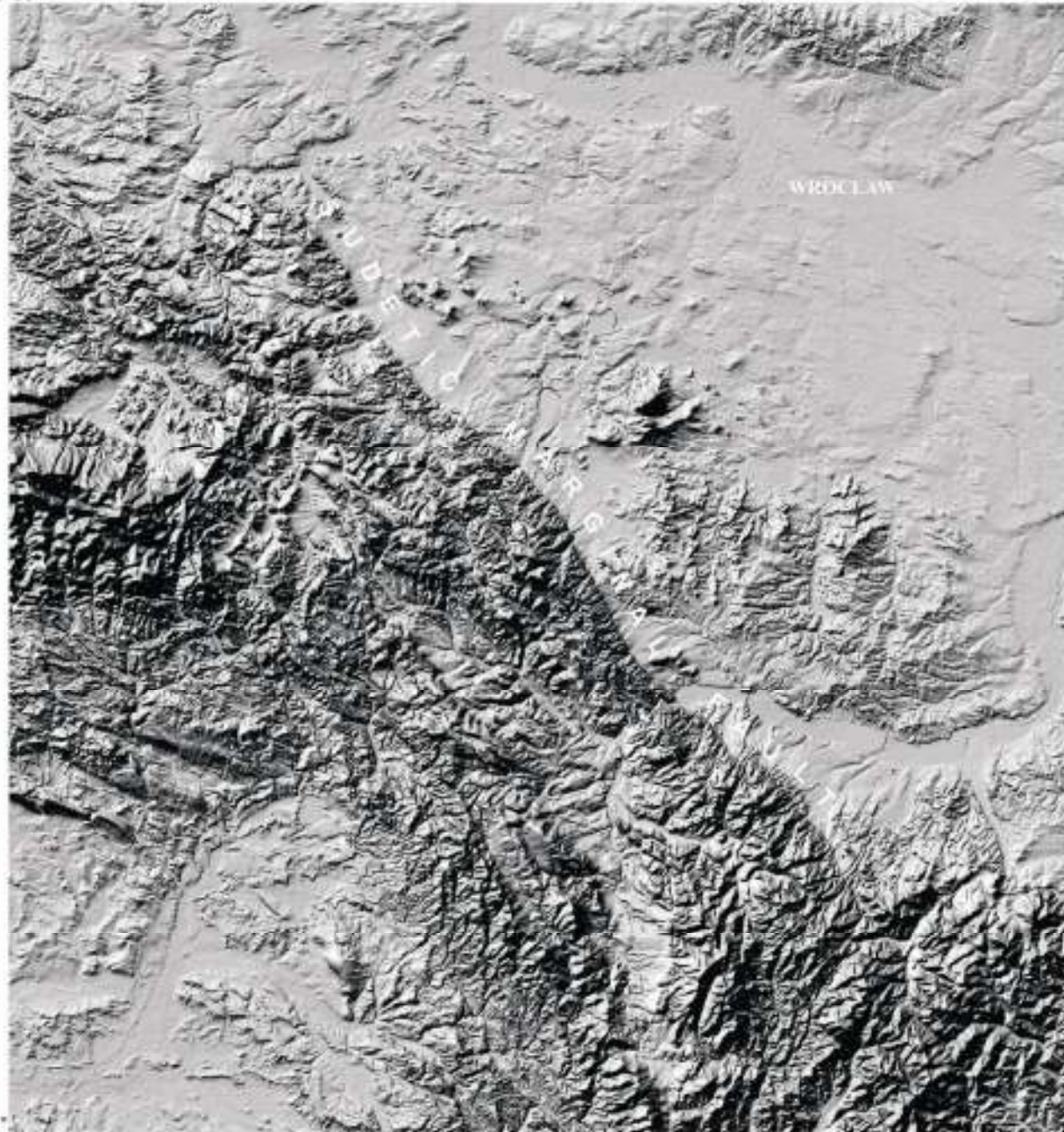
Typical values for the Basin-and-Range Province:

range: 0.05-47

average: 1.3-11.0

15°30'

51°
20'

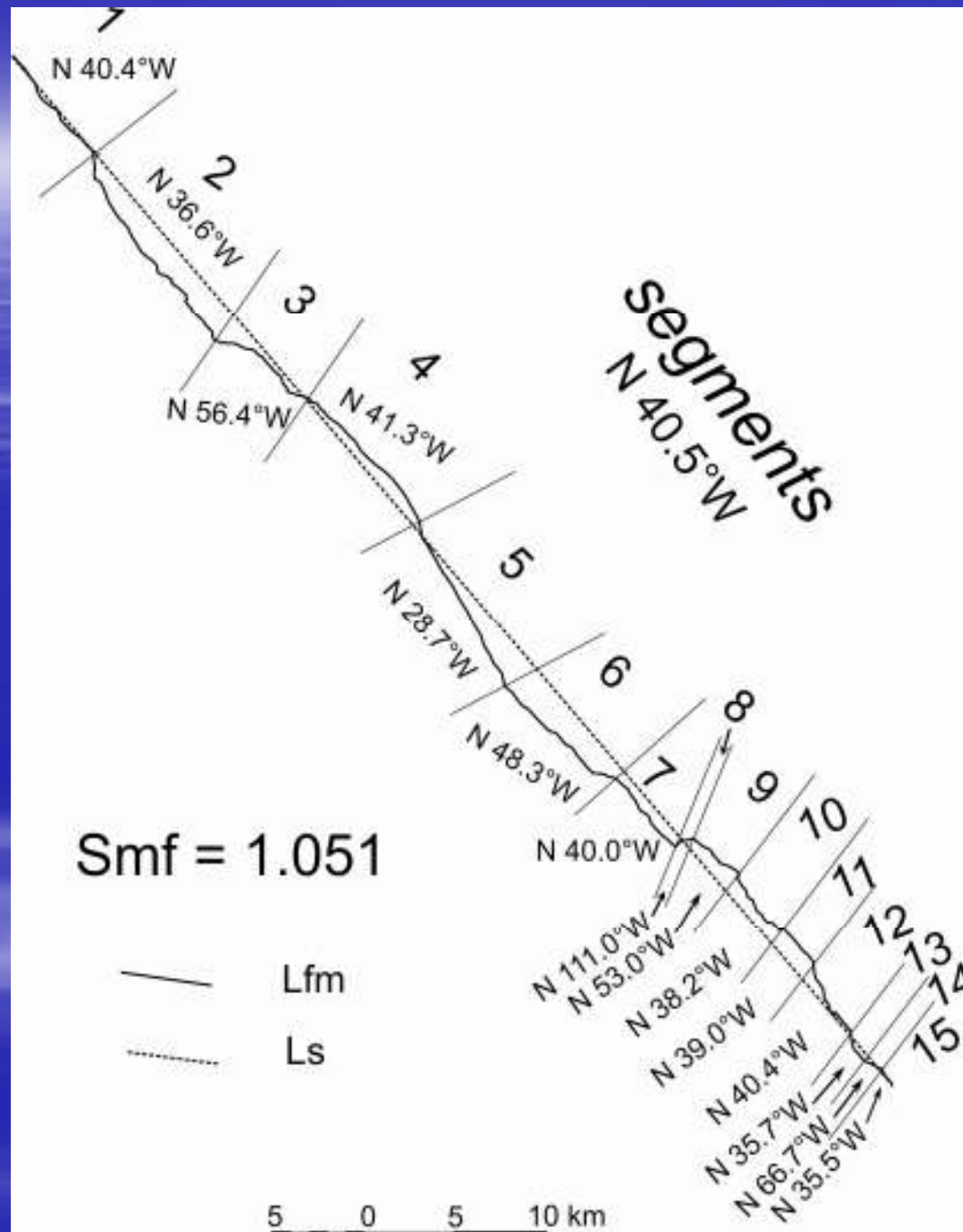


WROCLAW

51°
20'

0 25 km

17°30'



Individual fault segments bear a flight of two to five tiers of triangular facets, showing differentiated state of preservation and degree of erosional remodelling.

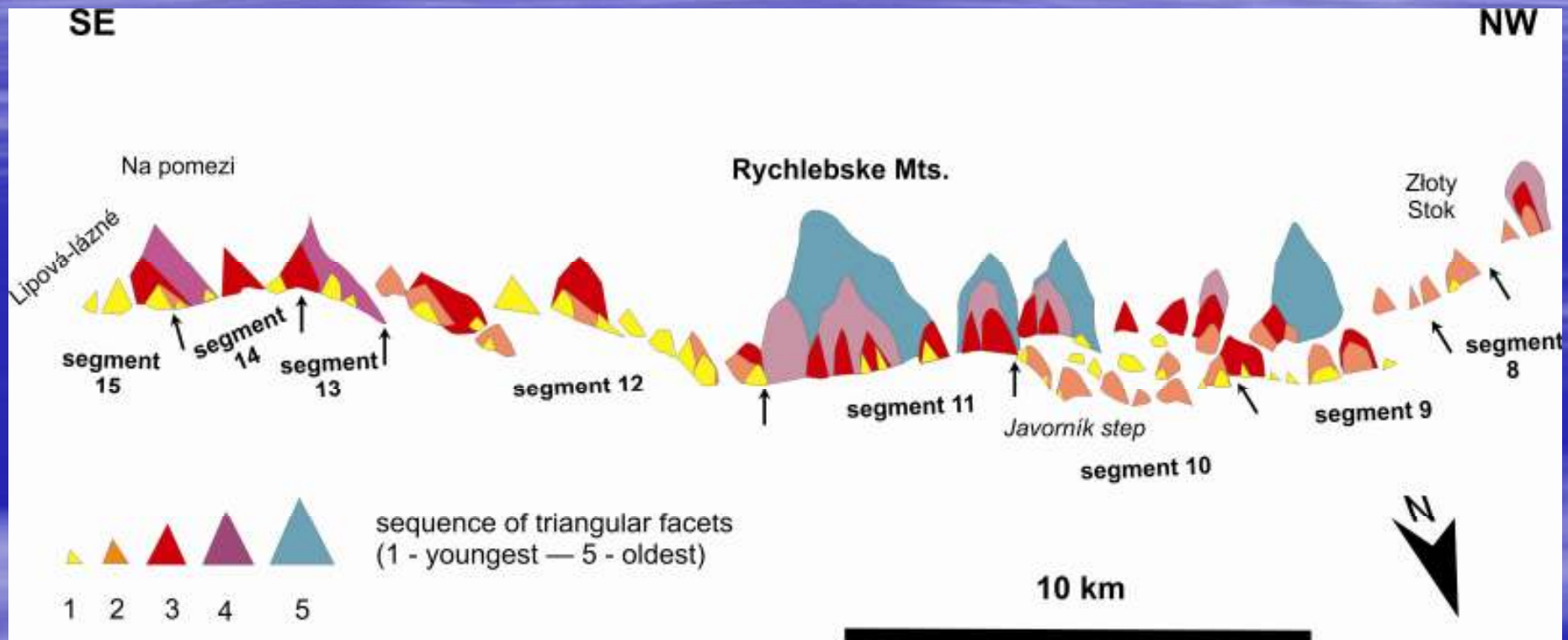
Average heights of these facets in the Czech portion of the fault are: 28 m, 60 m, 111 m, 173 m and 275 m for successively older generations, whereas their equivalents in the Polish segments are, respectively, 23-54 m, 56-120 m, 100-125 m, 135-230 m and 300 m.

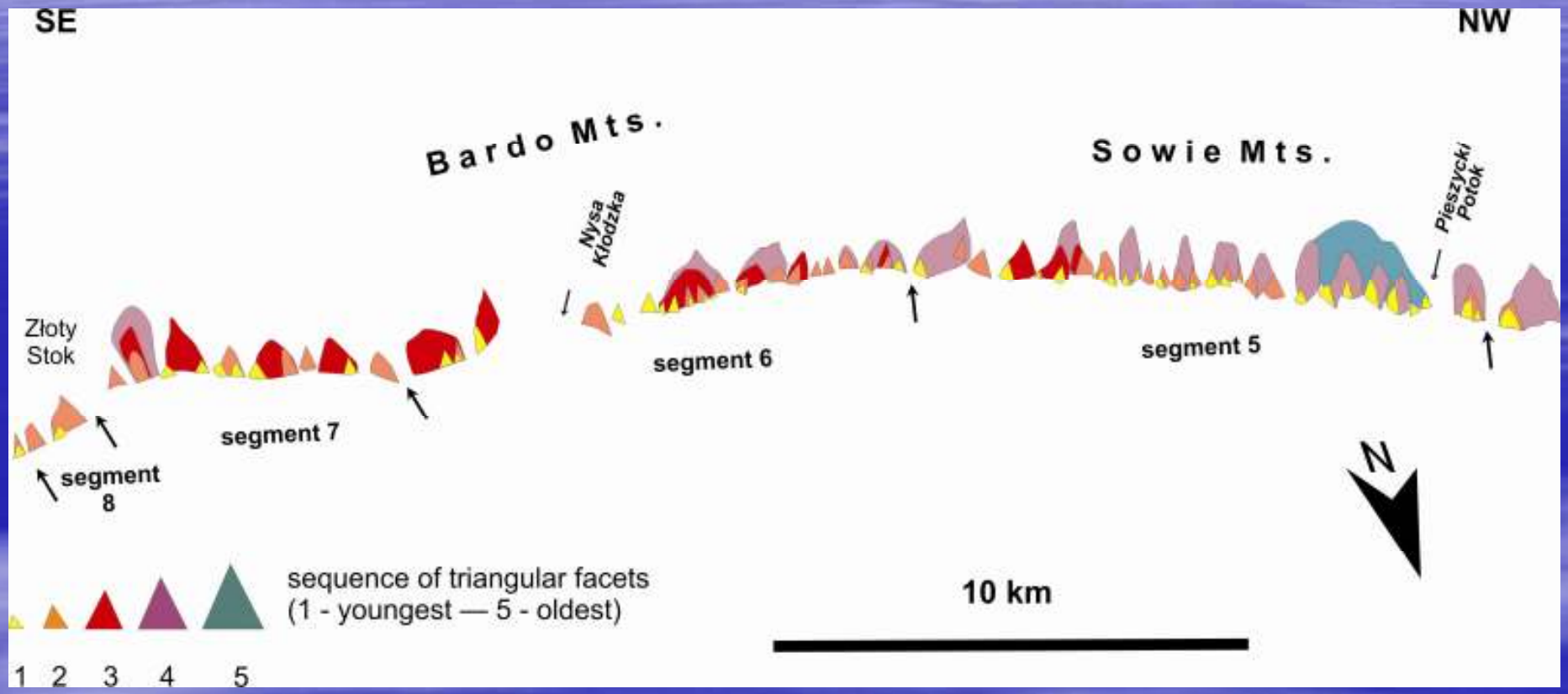
Discrete values are highly scattered: from 5 to 75 m in case of the youngest facets to 200-360 m within the oldest ones. The highest triangular facets are confined to Rychlebské (Złote) and Sowie Mts.

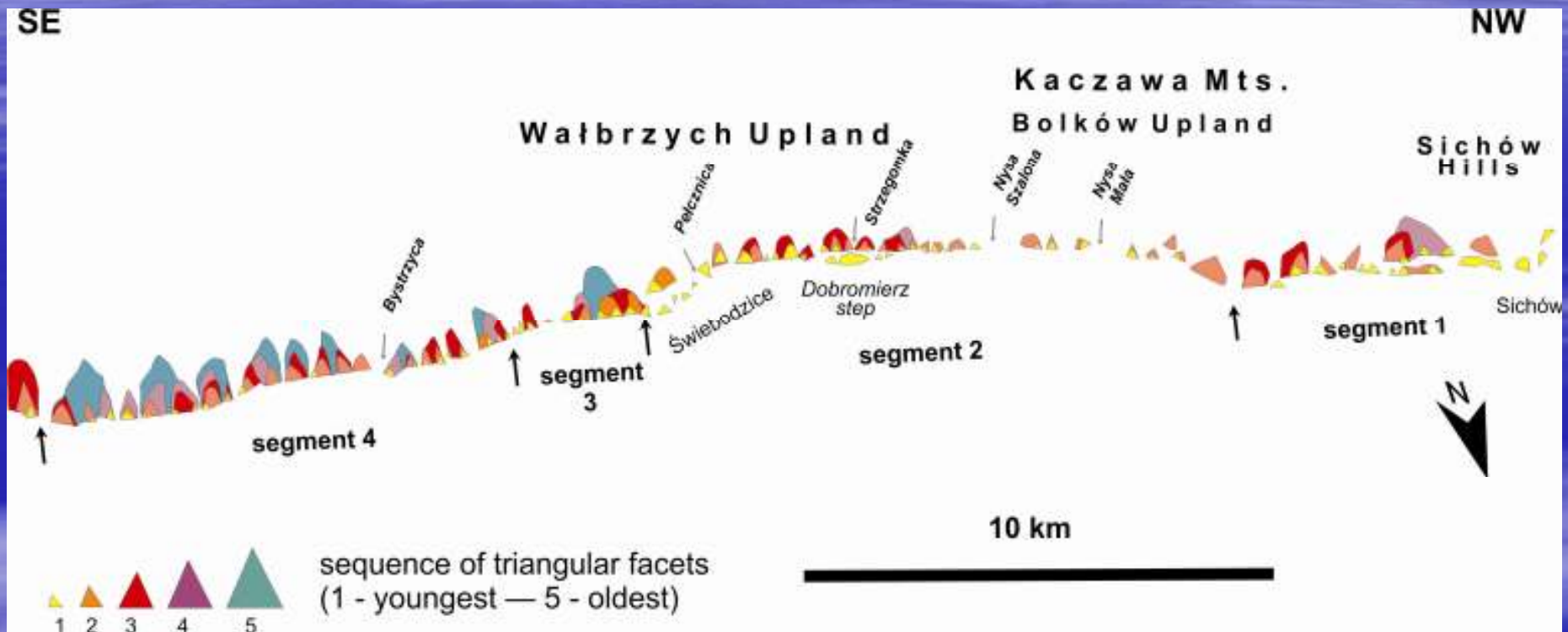
Tiering of triangular facets along the Sudetic Marginal Fault (minimum, maximum and average values in metres, values in brackets denote the number of facets per tier)

segment/tier	1	2	3	4	5
1	10-40 av. 24 (16)	40-90 av. 57 (6)	70-100 (3)	160 (1)	-
2	8-50 av. 24 (35)	30-105 av. 56 (23)	60-120 av. 92 (7)	100 (1)	-
3	8-45 av. 24 (11)	35-60 (3)	70-80 (2)	90 (1)	115-130 (2)
4	14-50 av. 36 (19)	30-110 av. 67 (21)	80-160 av. 118 (13)	110-210 av. 147 (7)	160-260 av. 199 (8)
5	30-100 av. 54 (23)	100-145 av. 120 (14)	180 (1)	180-270 av. 232 (9)	310 (1)
6	15-30 av. 23 (6)	45-100 av. 72 (8)	95-162 av. 125 (6)	130-135 (2)	-
7	19-42 av. 27 (6)	42-75 av. 56 (5)	110-141 av. 120 (4)	180 (1)	-
8	20 (1)	80-100 (2)	-	-	-
9	5-28 av. 16 (5)	40-80 av. 60 (5)	105 (1)	-	320 (1)
10	7-40 av. 18 (12)	30-80 av. 48 (8)	85-110 av. 102 (5)	160-210 (2)	220 (1)
11	55 (3)	-	80-110 av. 99 (6)	110-180 (3)	200-360 (2)
12	10-52 av. 28 (9)	40-100 av. 65 (7)	64-130 (3)	-	-
13	30 (1)	-	115 (1)	184 (1)	-
14	43-75 (2)	-	124-170 (2)	-	-
15	50-60 (2)	70-90 (2)	170 (1)	220 (1)	-

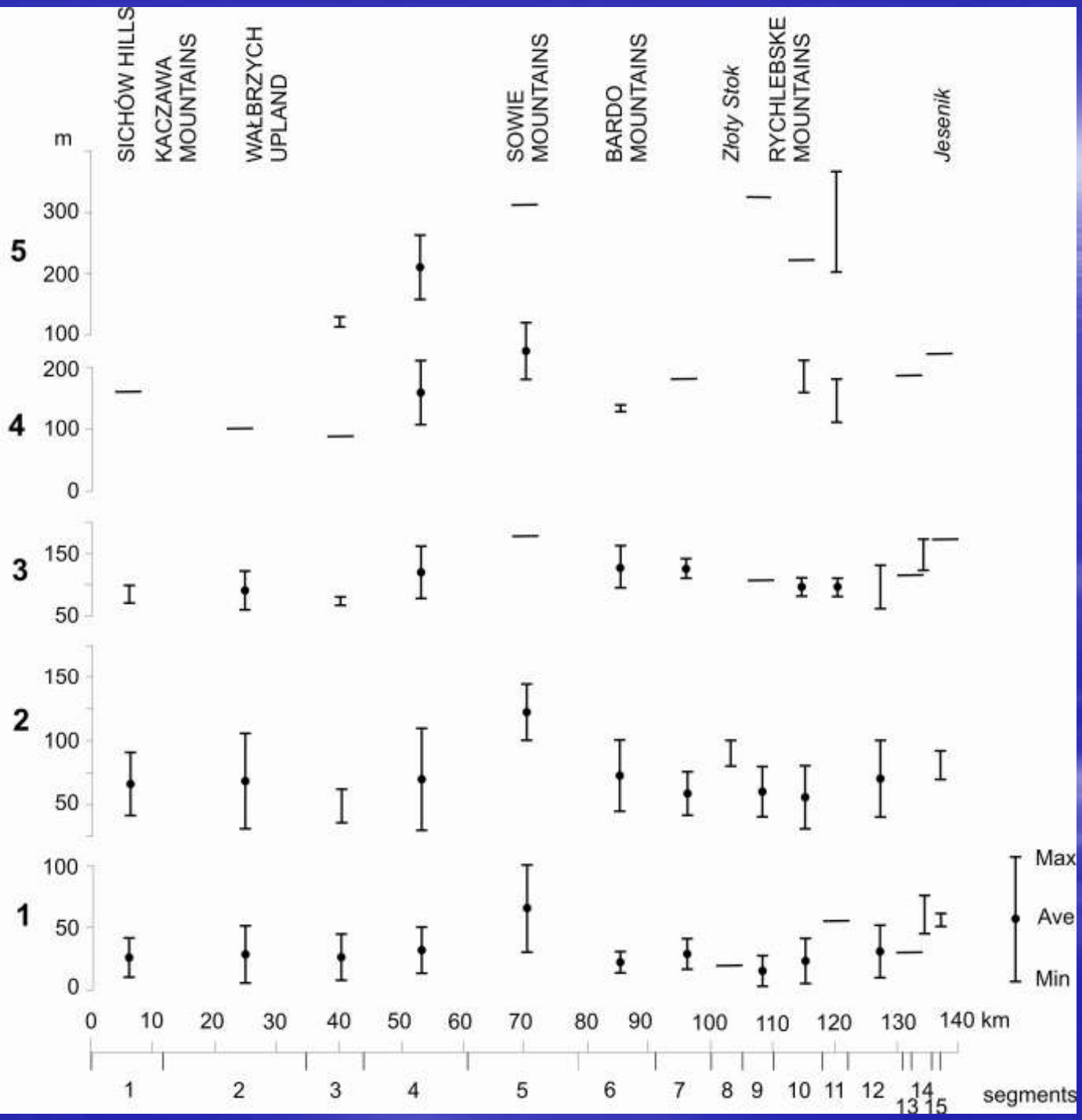
Polish part	8-100 av. 42 (84)	30-145 av. 71 (80)	60-162 av. 111 (36)	90-270 av. 178 (22)	115-310 av. 195 (11)
Czech part	5-75 av. 28 (35)	30-100 av. 60 (24)	64-170 av. 111 (19)	110-220 av. 173 (7)	200-360 av. 275 (4)







TIERS OF TRIANGULAR FACETS

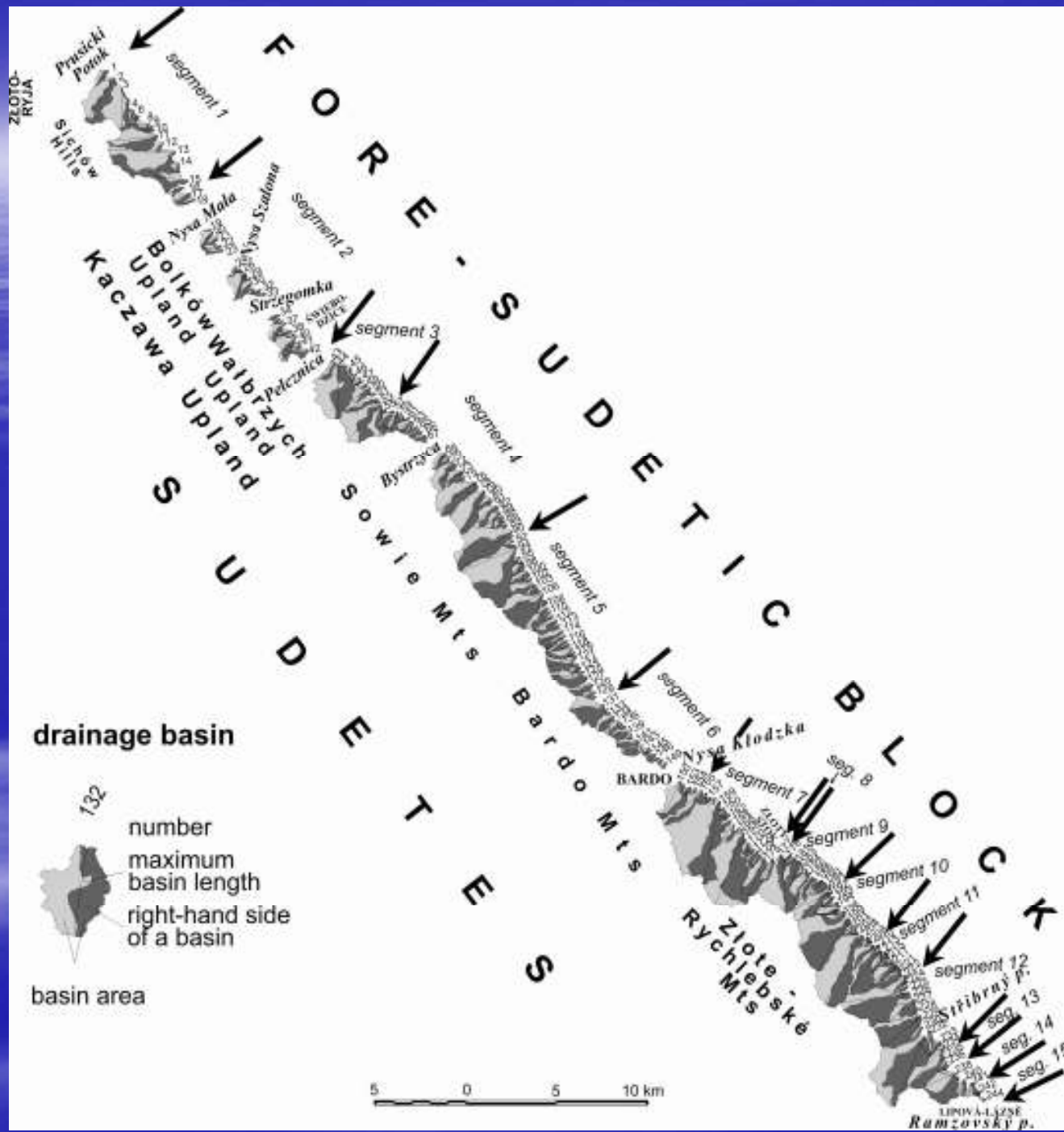


segments

This tiering points to at least five episodes of uplift of the SMF footwall, probably starting shortly after 31 Ma, i.e. postdating basalts of the Sichów Hills area that are displaced by the fault.

More detailed age constraints are provided by the results of apatite fission-track dating of the Sowie Mts. gneisses, pointing to rapid cooling and uplift after 7-5 Ma on either side of the fault (Aramowicz *et al.*, 2006).

These data suggest Pliocene and younger ages of the highest triangular facets that accompany the Sudetic mountain front. The age of younger uplift episodes is difficult to constrain due to the lack of datable marker sediments.



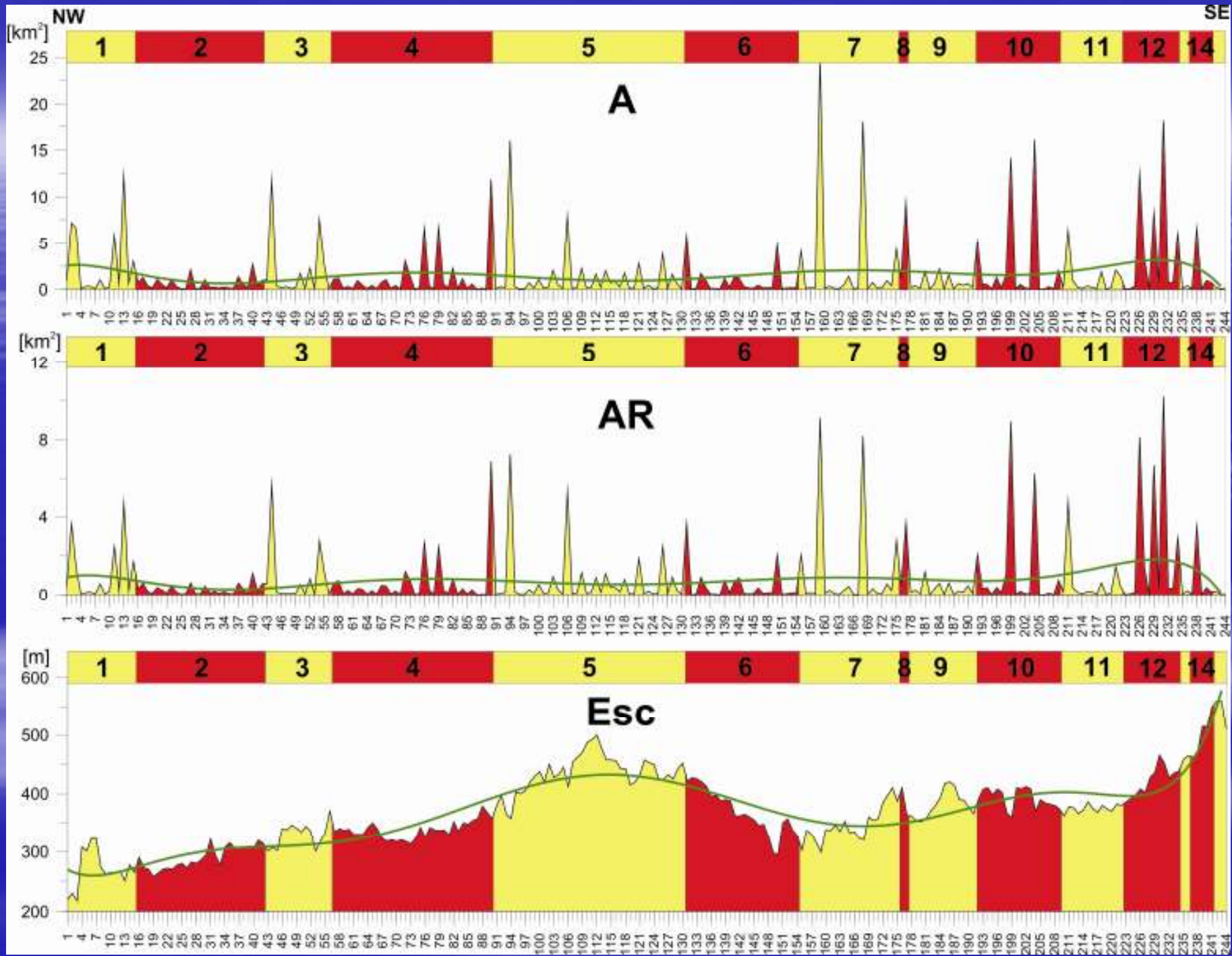
**Parameters describing small catchment areas along
the Sudetic Marginal Fault**

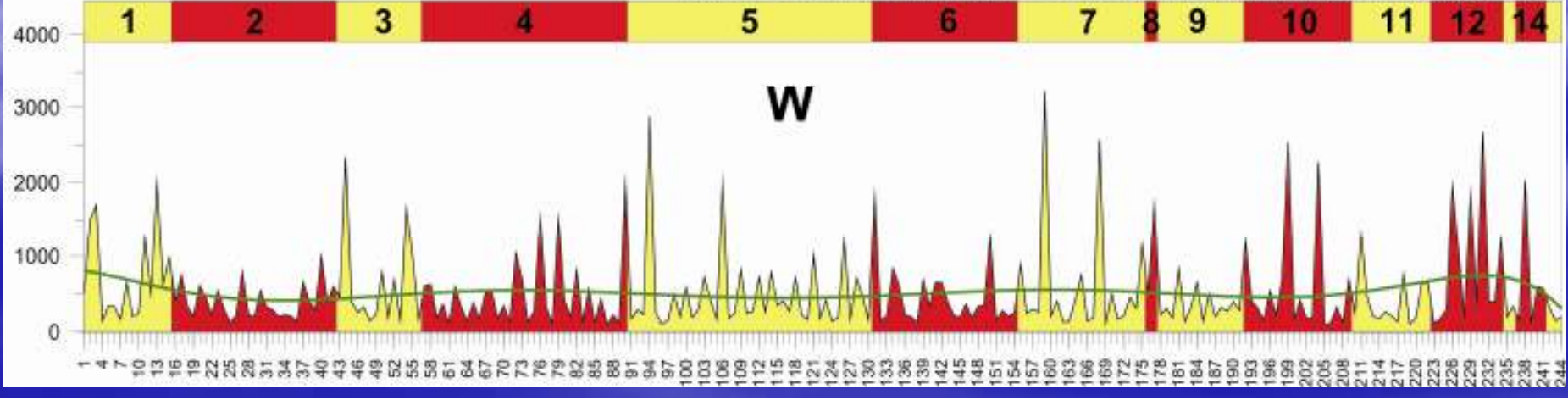
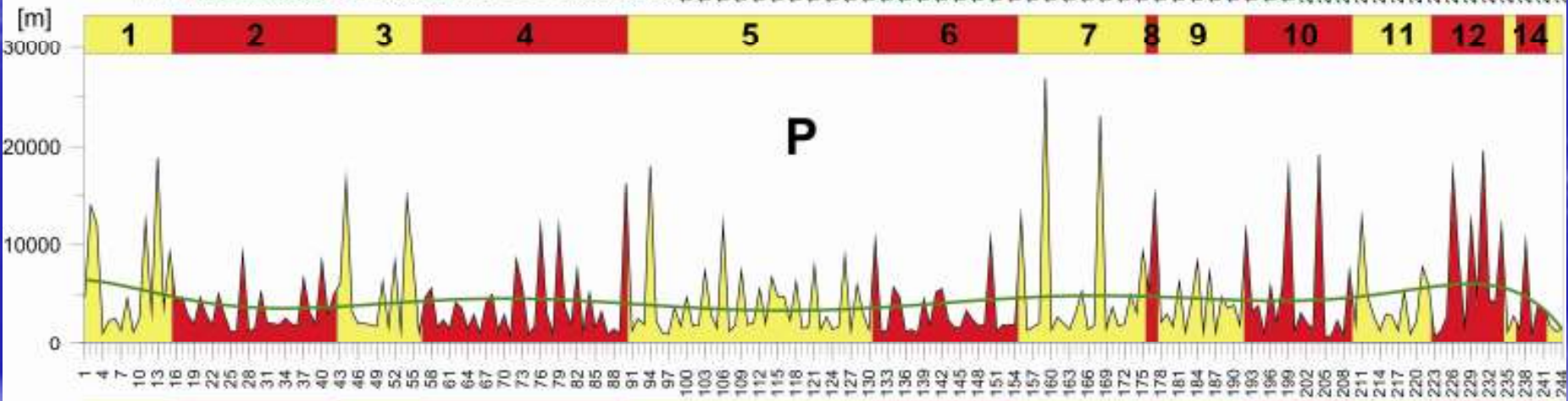
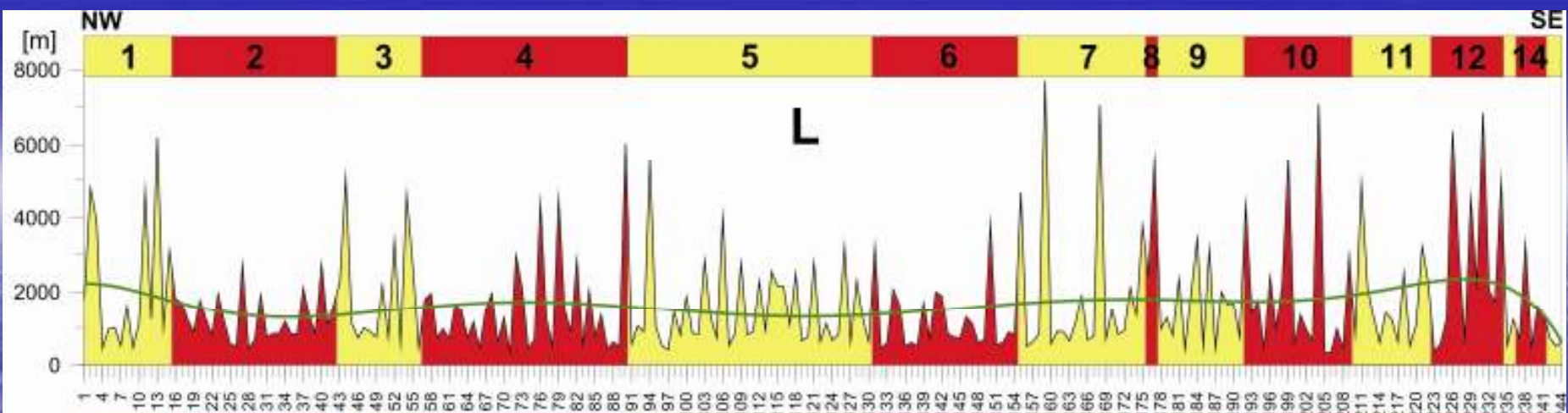
Parameter	Symbol	Formula	References
total area	A		Horton (1945)
area of the basin to the right (facing downstream) of the trunk stream	AR		
asymmetry factor	Af	100(AR/A)	Hare and Gardner (1985)
maximum basin length	L		Horton (1945), Schumm (1954)
basin perimeter	P		Smith (1950)
mean width of the basin	W	A/L	
maximum relief	H	Hmax-Hmin	Strahler (1954), Schumm (1954)
basin elongation ratio	Re	2(A/π)^{0.5}/L	Schumm (1956)
form ratio	Rf	A/L²	Horton (1945)
circulatory ratio	Rk	(4πA)/P²	Miller (1953), Gregory and Walling (1973)
relief ratio	Rh	H/L	Schumm (1954, 1956)
relative relief	Rhp	H/P	Melton (1957, 1958)

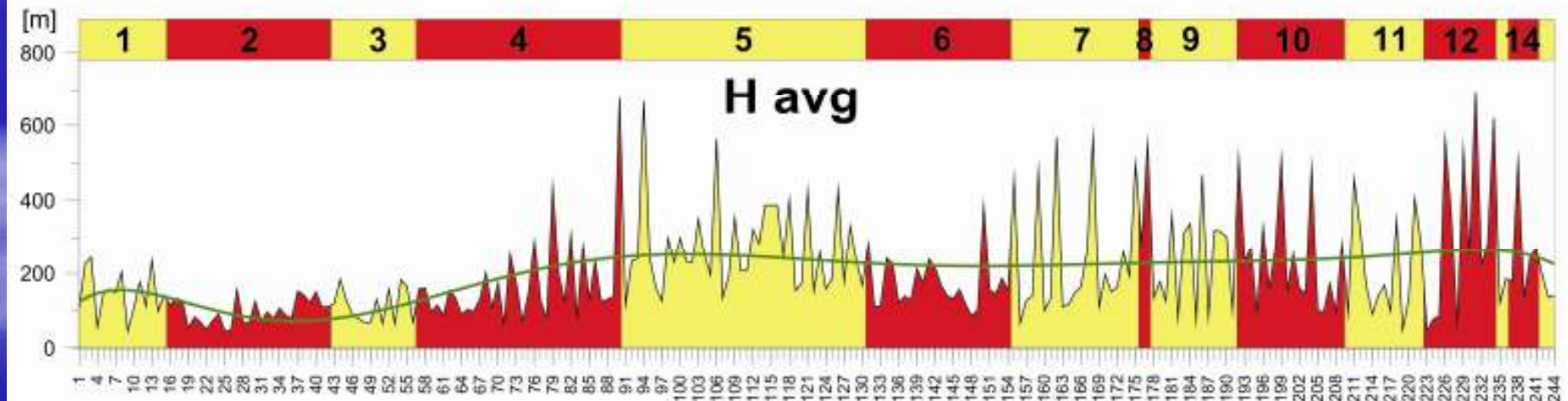
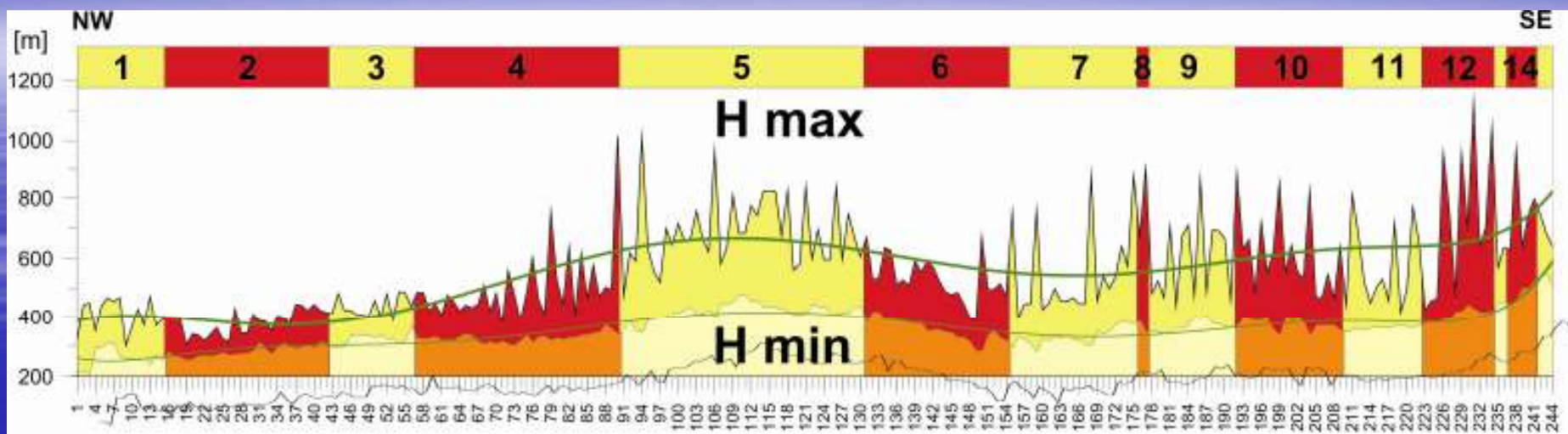
Morphometric parameters of 244 small (0.03-24.8 sq. km, av. 1.61 sq. km) catchment areas of streams that dissect the fault scarp include, *i.a.* elongation, relief, and average slope of individual catchment areas, together with values of the valley floor width to valley height ratios.

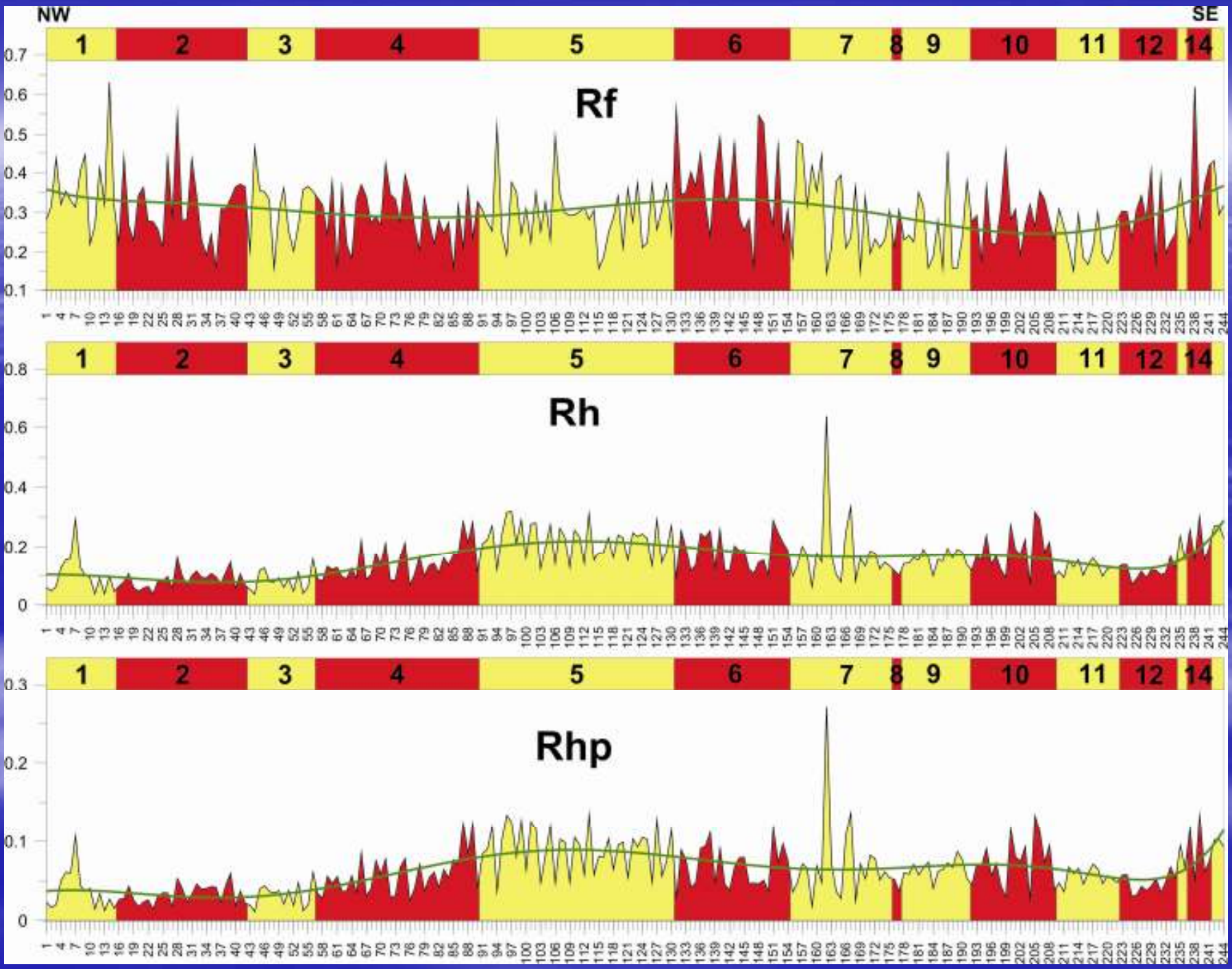
The relief energy values range between 45 m and 695 m, averaging 202 m, basin elongation ratios are between 0.43 and 0.90 (av. 0.61), and valley floor width-valley height ratios change between 0.04 and 9.45, averaging 0.83.

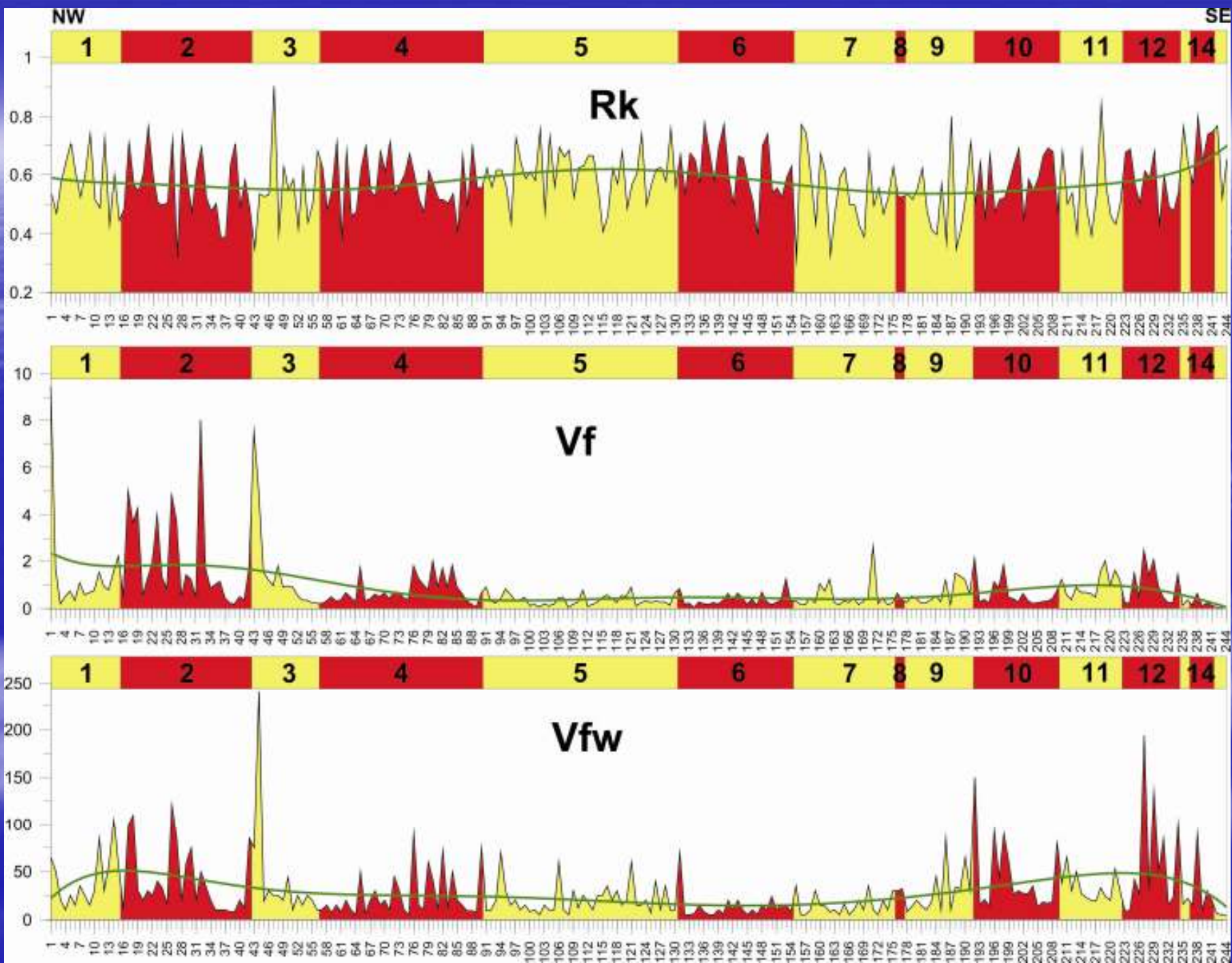
Parameter (n = 244)	average	max	min
L [km]	1.656	7.708	0.294
A [km²]	1.614	24.820	0.026
AR [km²]	0.782	10.223	0.015
Af [%]	48.53	80.77	15.42
P [km]	4.415	26.863	0.749
W [km]	0.520	3.220	0.082
Hmax [m a.s.l.]	554.9	1125.0	302.5
Hmin [m a.s.l.]	355.5	550.0	207.0
H [m]	201.5	695.0	44.5
Re	0.61	0.90	0.43
Rf	0.30	0.63	0.15
Rk	0.58	0.90	0.32
Rh	0.15	0.64	0.04
Rhp	0.06	0.27	0.01
k	14.42	27.25	6.34
Vfw [m]	29	240	5
Esc [m a.s.l.]	367.4	560.0	217.5
Eld [m a.s.l.]	419.8	765.0	223.8
Erd [m a.s.l.]	418.9	730.0	230.0
Vf	0.83	9.45	0.04

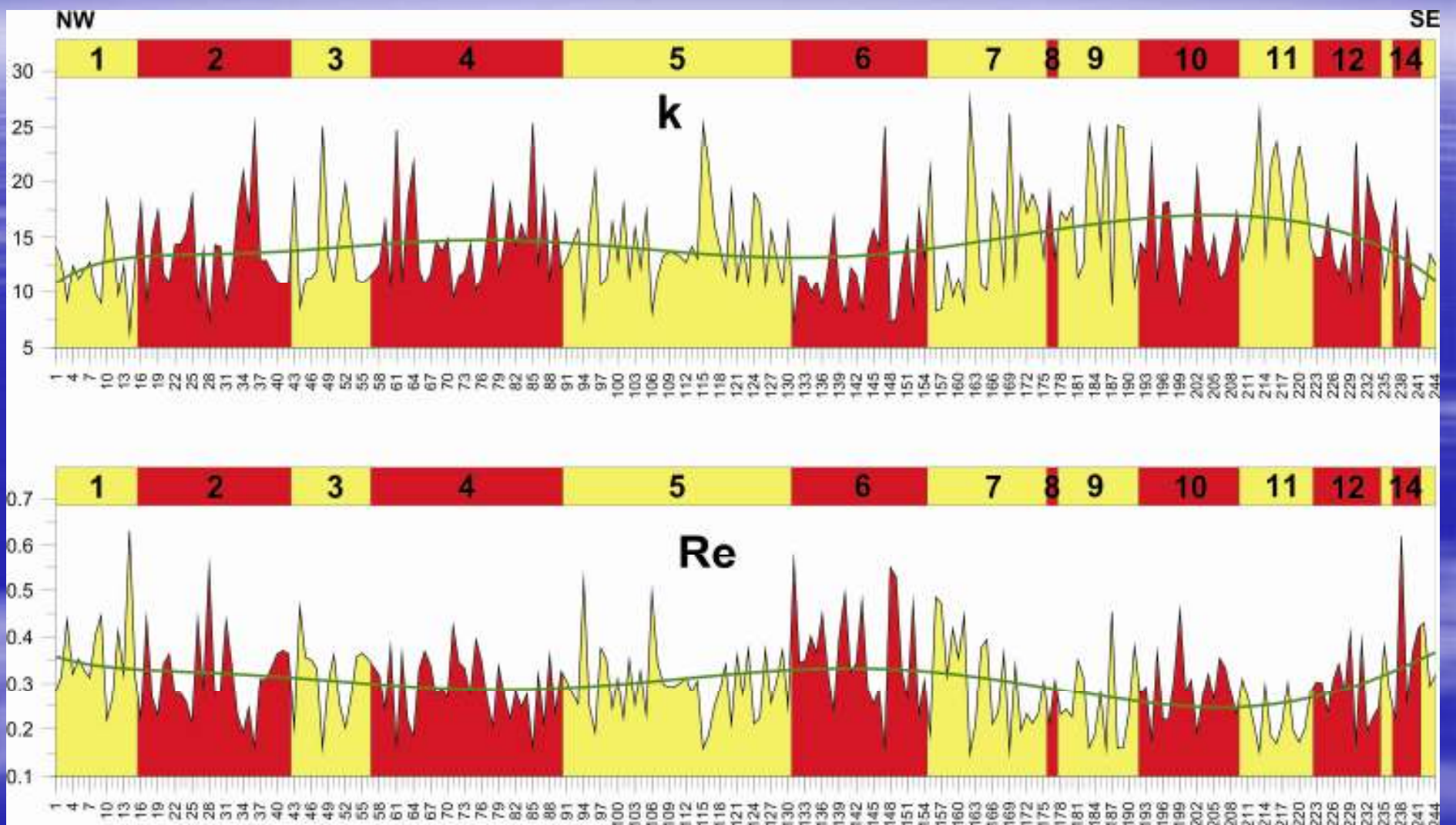


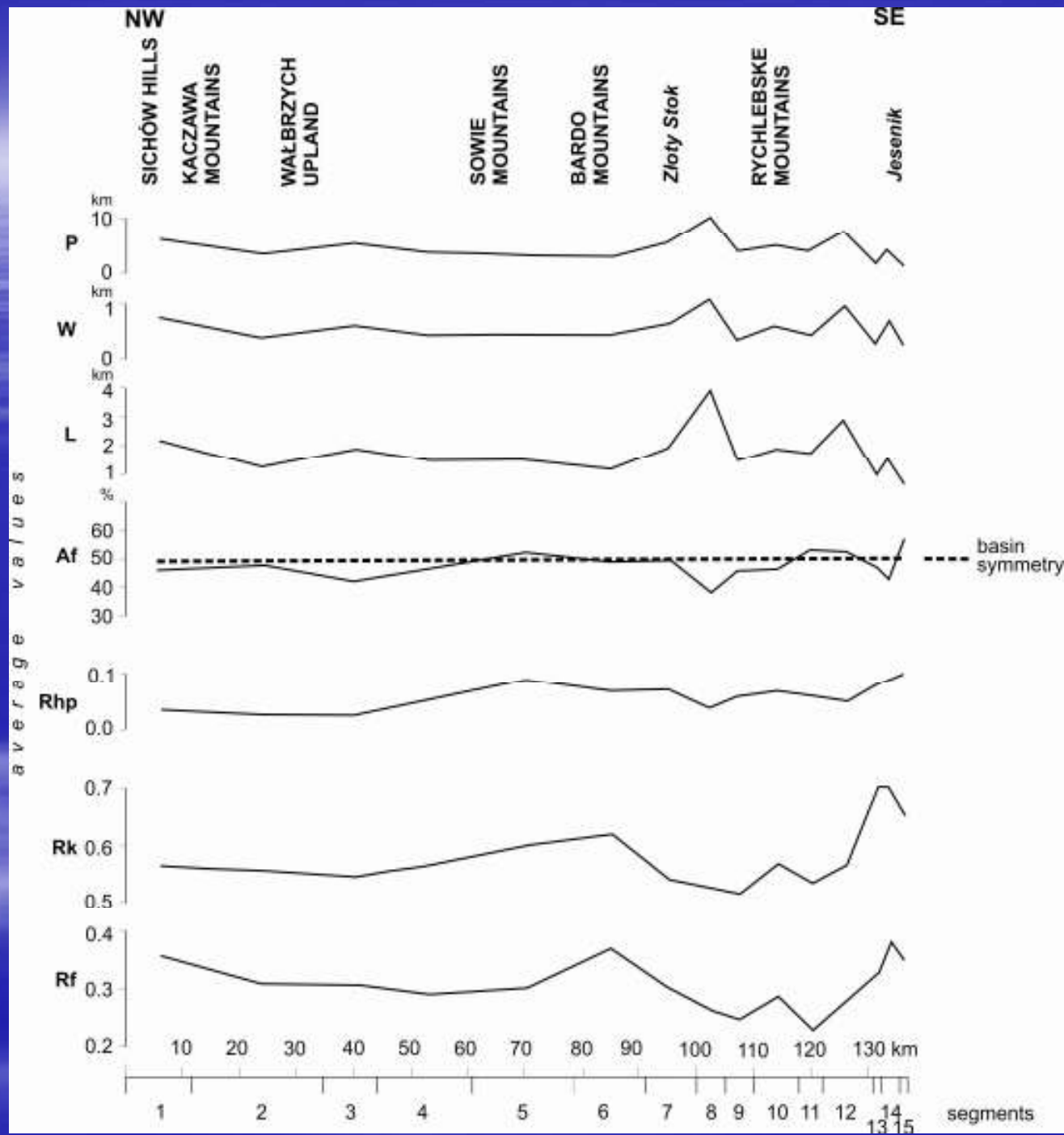


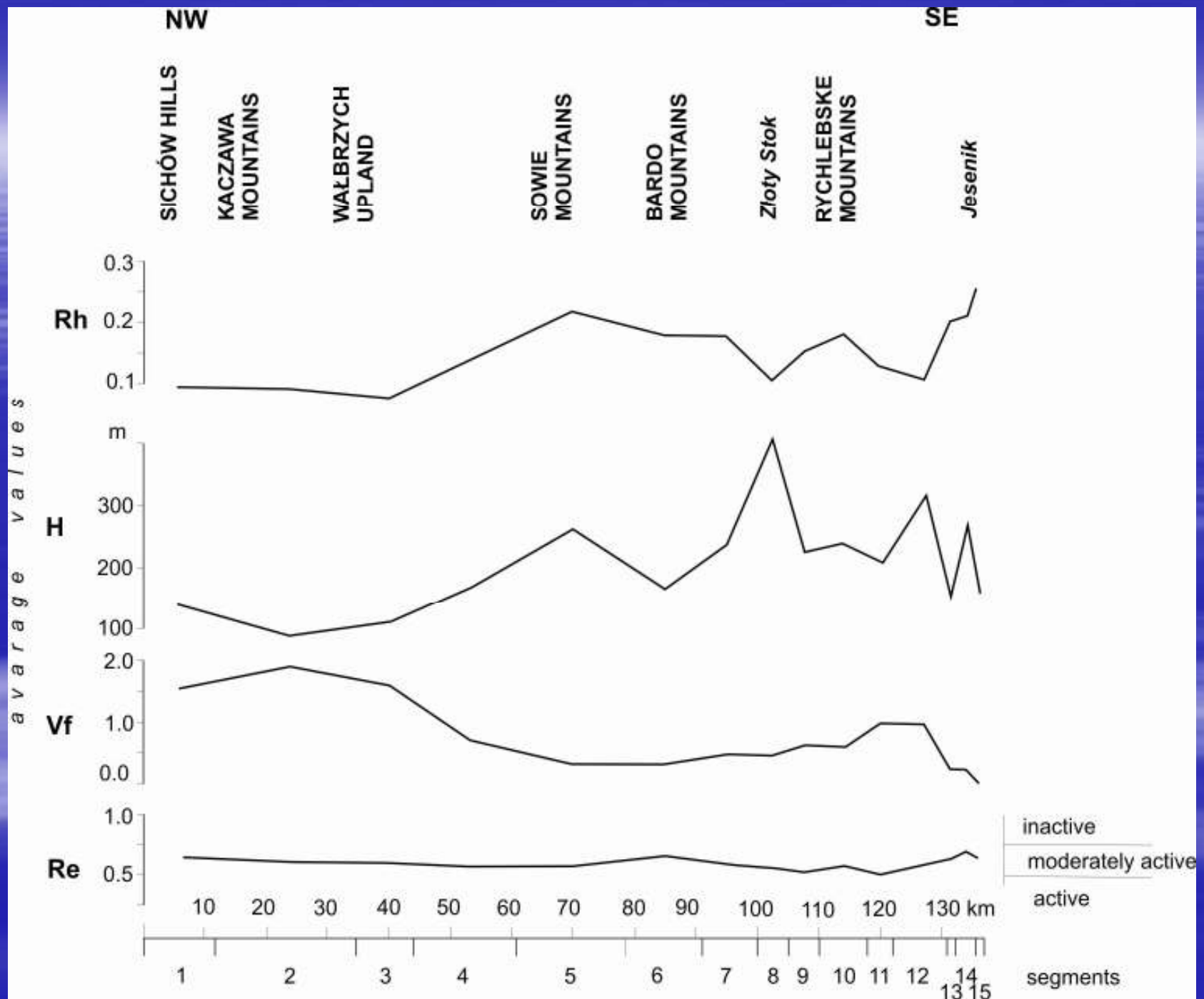








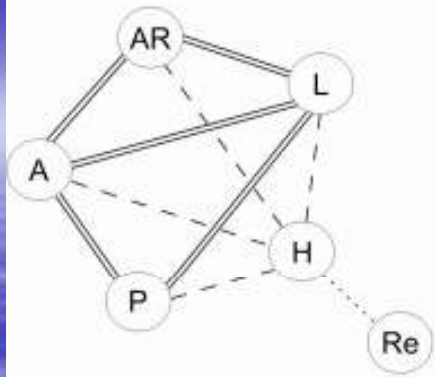




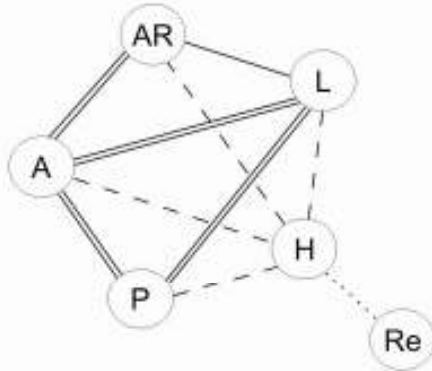
Correlation coefficients among individual drainage basin parameters within segments of the Sudetic Marginal Fault

Segment #	Re-H	L-H	A-L	P-H	A-P	AR-A	A-H	AR-L	L-P	AR-H
1 (n = 15)	-.107	.767	.968	.776	.980	.957	.756	.960	.995	.698
2 (n = 27)	.057	.738	.948	.738	.968	.966	.691	.917	.982	.693
3 (n = 14)	.409	.931	.913	.921	.950	.990	.793	.875	.991	.750
4 (n = 34)	.233	.929	.950	.921	.950	.977	.927	.898	.998	.910
5 (n = 40)	.437	.966	.872	.948	.928	.982	.825	.885	.990	.848
6 (n = 24)	.069	.936	.931	.915	.960	.979	.849	.883	.991	.776
7 (n = 21)	-.190	.759	.935	.719	.970	.990	.637	.959	.992	.687
8 (n = 2)
9 (n = 14)	-.637	.925	.920	.906	.952	.885	.788	.748	.994	.737
10 (n = 18)	.200	.941	.938	.931	.961	.965	.817	.875	.993	.787
11 (n = 13)	.218	.954	.945	.930	.958	.979	.825	.893	.995	.736
12 (n = 12)	.420	.970	.940	.954	.965	.983	.876	.924	.995	.858
13 (n = 2)
14 (n = 5)
15 (n = 3)
1-15 (n=244)	.035	.784	.909	.741	.944	.966	.686	.887	.988	.720

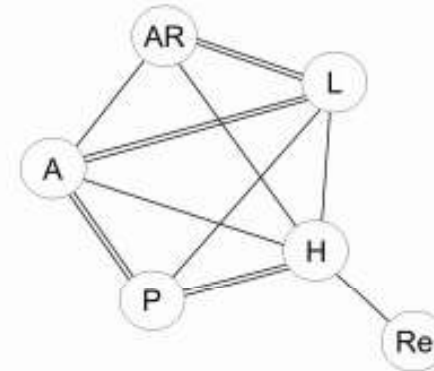
segment 1



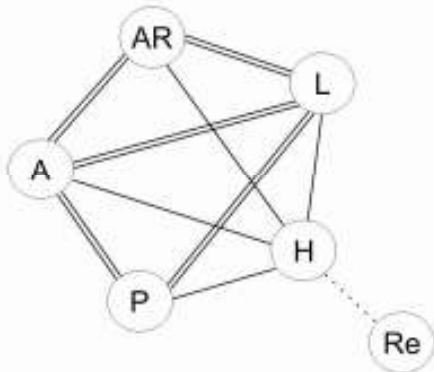
segment 2



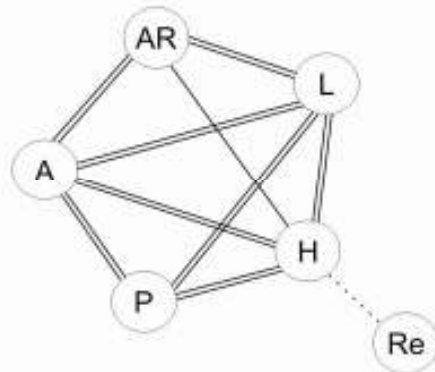
segment 3



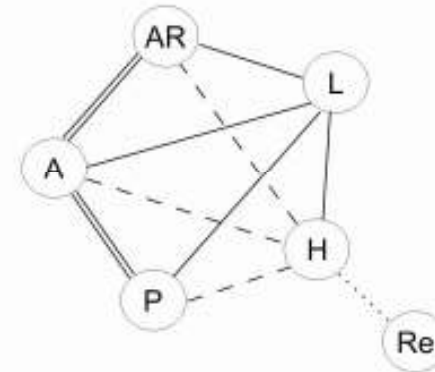
segment 4



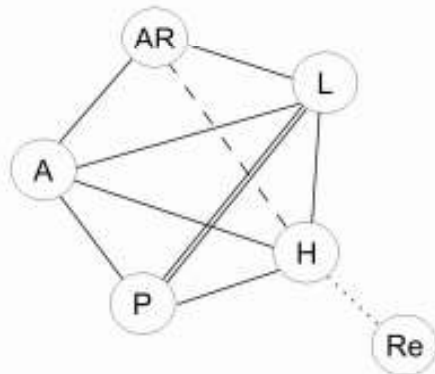
segment 5



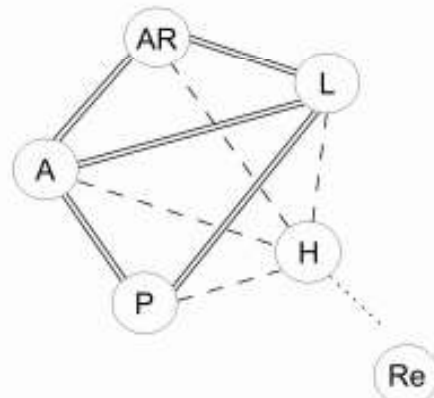
segment 6







segment 7

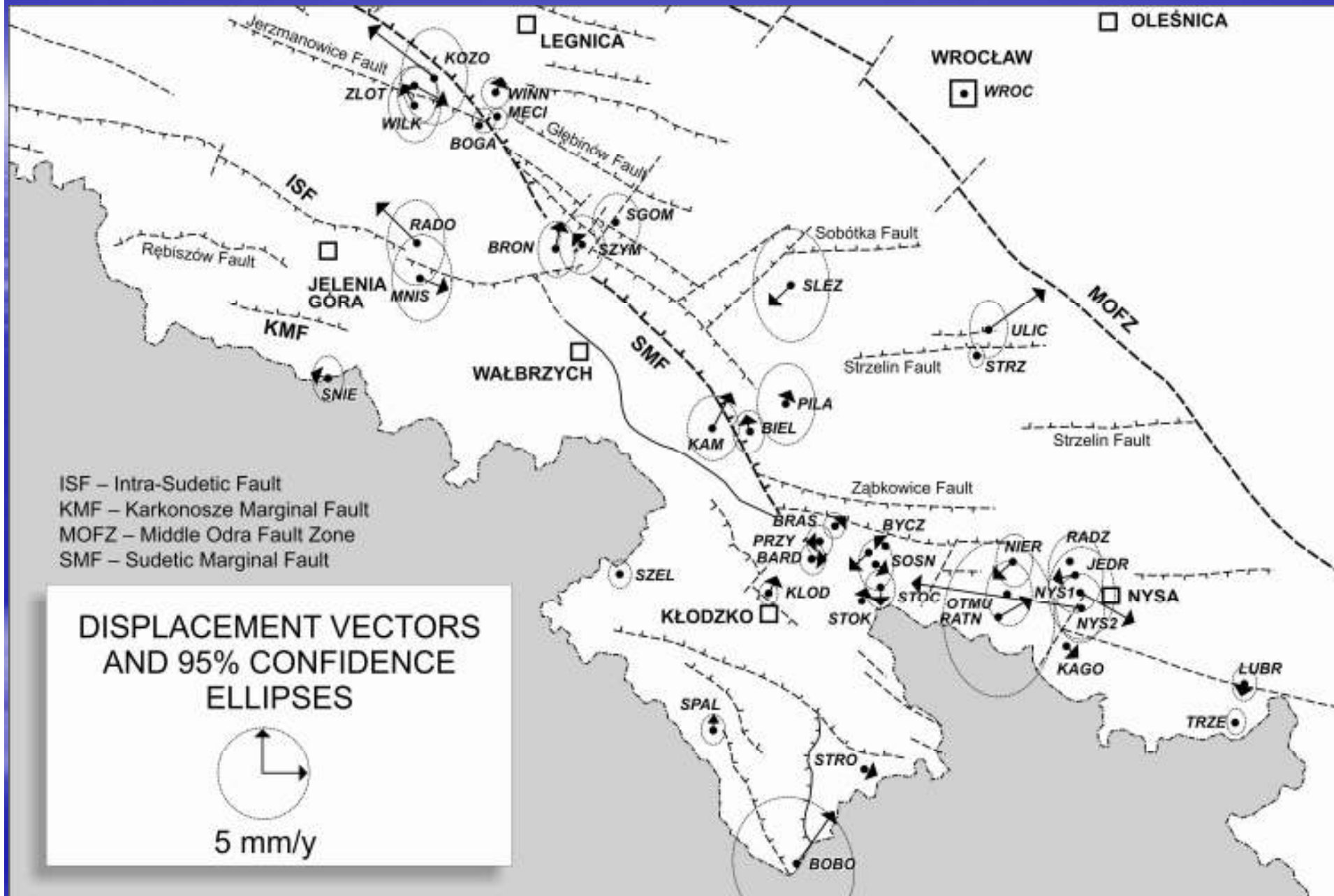


segments 1-7



correlation coefficients

-  > 0.95
-  0.80-0.95
-  0.55-0.80
-  < 0.55



OLEŚNICA

WROCLAW
WROC

LEGNICA

Jerzmanowice Fault
KOZO
ZLOT
WILK
WINN
MECI
BOGA

Glebinów Fault

ISF

Rębiszów Fault

KMF

SNIE

RADO

MNIS

JELENIA GÓRA

WALSBRZYCH

BRON

SMF

SZYM

Sobótka Fault

SLEZ

Strzelin Fault

ULIC

STRZ

MOFZ

Strzelin Fault

PILA

KAM

BIEL

Ząbkowice Fault

BRAS

BYCZ

PRZY
BARD

SOSN

NIER

RADZ

JEDR

SZEL

KŁOD

STOC

OTMU
RATN

NYS1

NYS2

NYSA

KŁODZKO

STOK

KAGO

LUBR

TRZE

SPAL

STRO

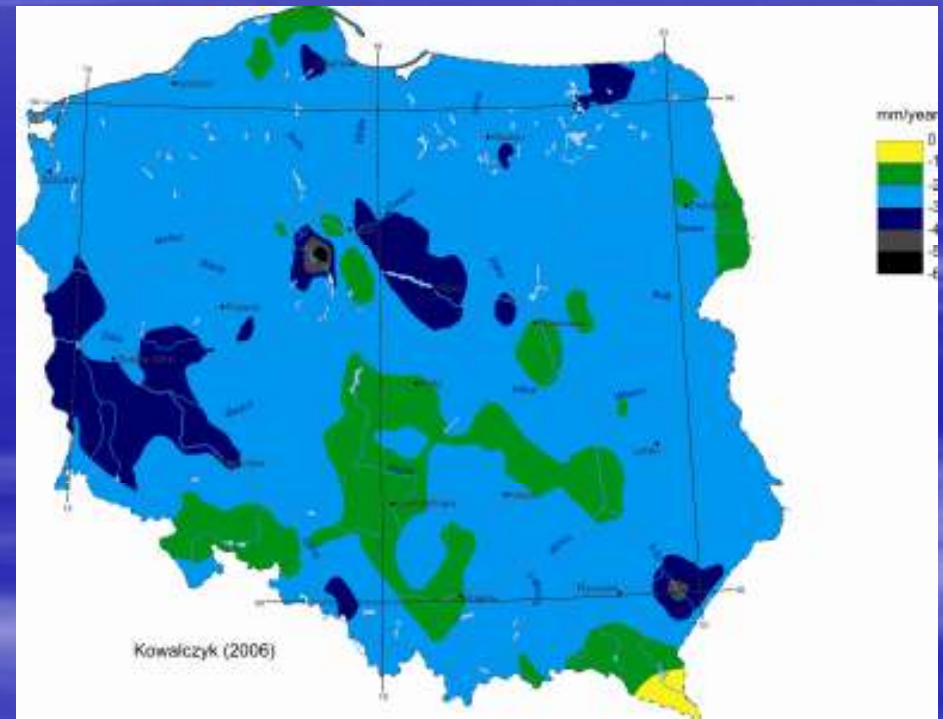
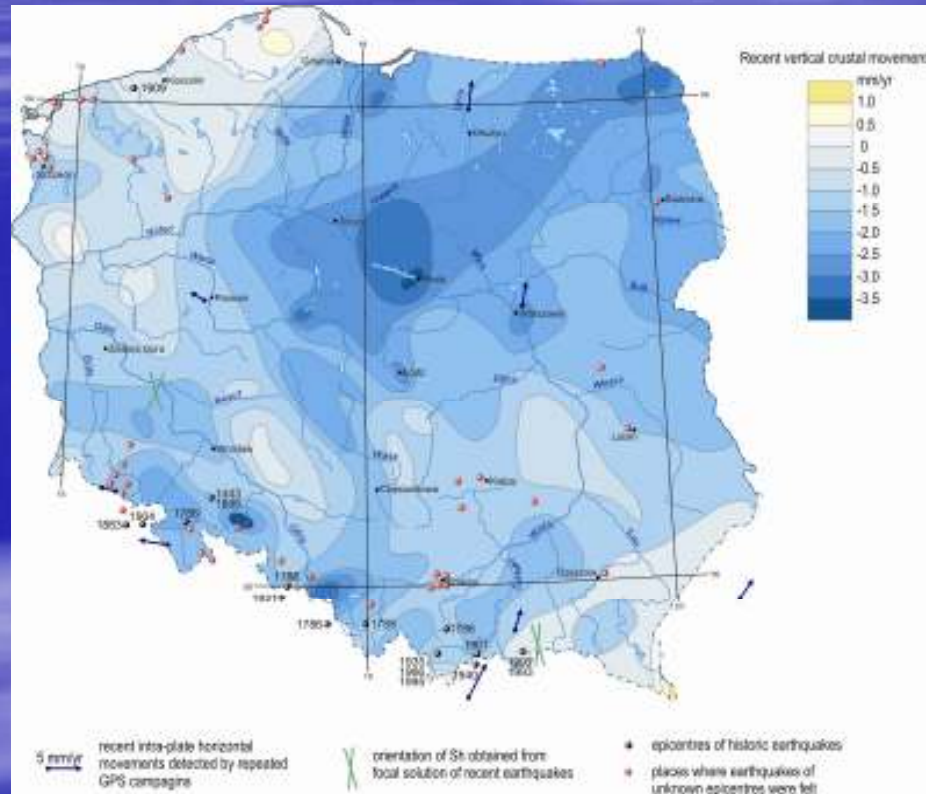
BOBO

Rates of vector relative elongation and rotation on the profiles

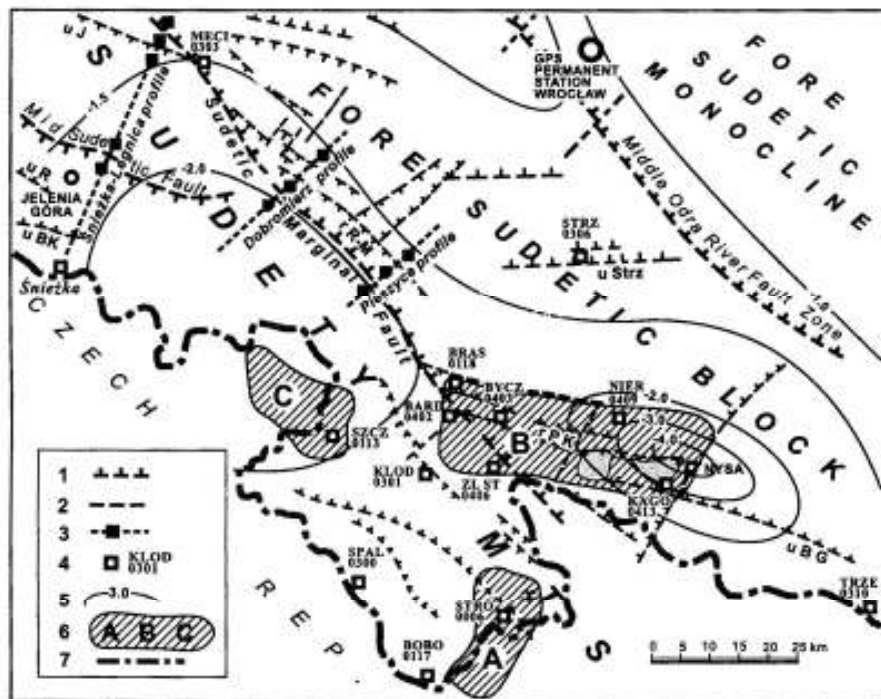
PROFILE	FROM	TO	ε_{AB} (mm/10km/ yr)	$\sigma_{\varepsilon_{AB}}$ (mm/10km/ yr)	RATIO	$\widehat{\omega}_{AB}$ (rad/year)	$\sigma_{\widehat{\omega}_{AB}}$ (rad/year)	RATIO
A	ZLOT	KOZO	-4.65	8.04	-0.6	-3.56E-06	7.54E-07	-4.7
A	WILK	ZLOT	-7.18	21.14	-0.3	4.35E-06	1.65E-06	2.6
B	BOGA	MECI	-4.72	4.14	-1.1	3.04E-08	4.78E-07	0.1
B	MECI	WINN	5.81	3.13	1.9	2.80E-07	2.95E-07	0.9
C	BRON	SZYM	-4.11	5.14	-0.8	4.85E-07	6.33E-07	0.8
C	SZYM	SGOM	0.48	3.59	0.1	3.24E-07	3.69E-07	0.9
D	KAMI	BIEL	-4.03	3.33	-1.2	3.65E-07	4.11E-07	0.9
D	BIEL	PILA	0.57	3.17	0.2	1.19E-07	3.38E-07	0.4
E	BARD	PRZY	1.05	7.83	0.1	-1.33E-06	6.71E-07	-2.0
E	KLOD	BARD	-1.26	0.92	-1.4	1.68E-07	9.09E-08	1.9
E	PRZY	BRAS	4.00	2.86	1.4	1.82E-07	2.85E-07	0.6
F	STOK	STOO	-4.08	4.80	-0.9	6.96E-07	5.41E-07	1.3
F	STOO	SOSN	1.25	4.01	0.3	2.83E-07	3.15E-07	0.9
F	SOSN	BYCZ	1.89	5.14	0.4	-8.41E-07	4.40E-07	-1.9

ε_{AB} - vector relative elongation, $\widehat{\omega}_{AB}$ - average angle of rotation

Recent vertical crustal movements



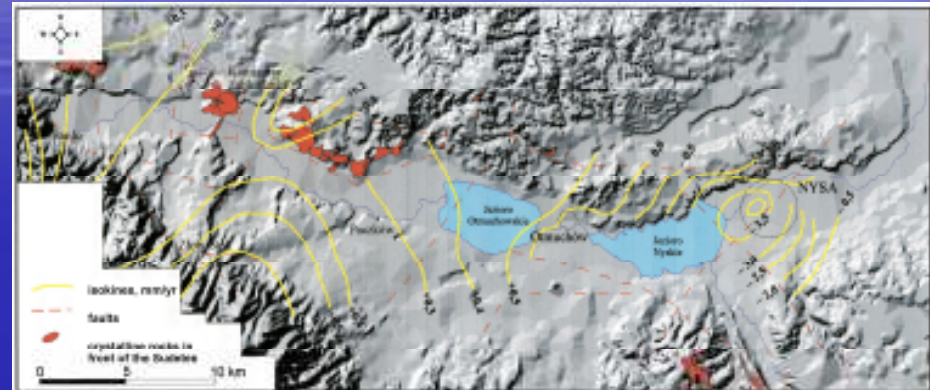
Recent vertical crustal movements



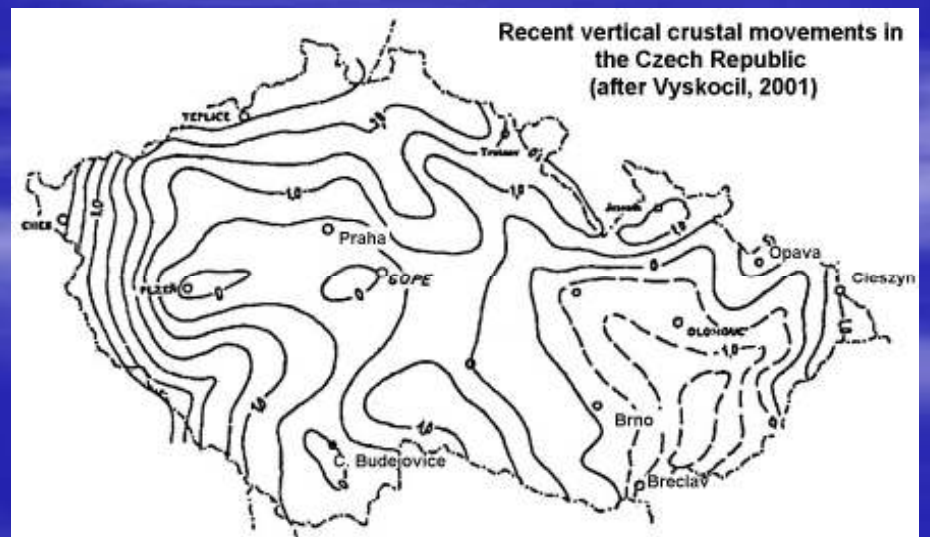
Sketch map of geological structure of the Polish Sudetes

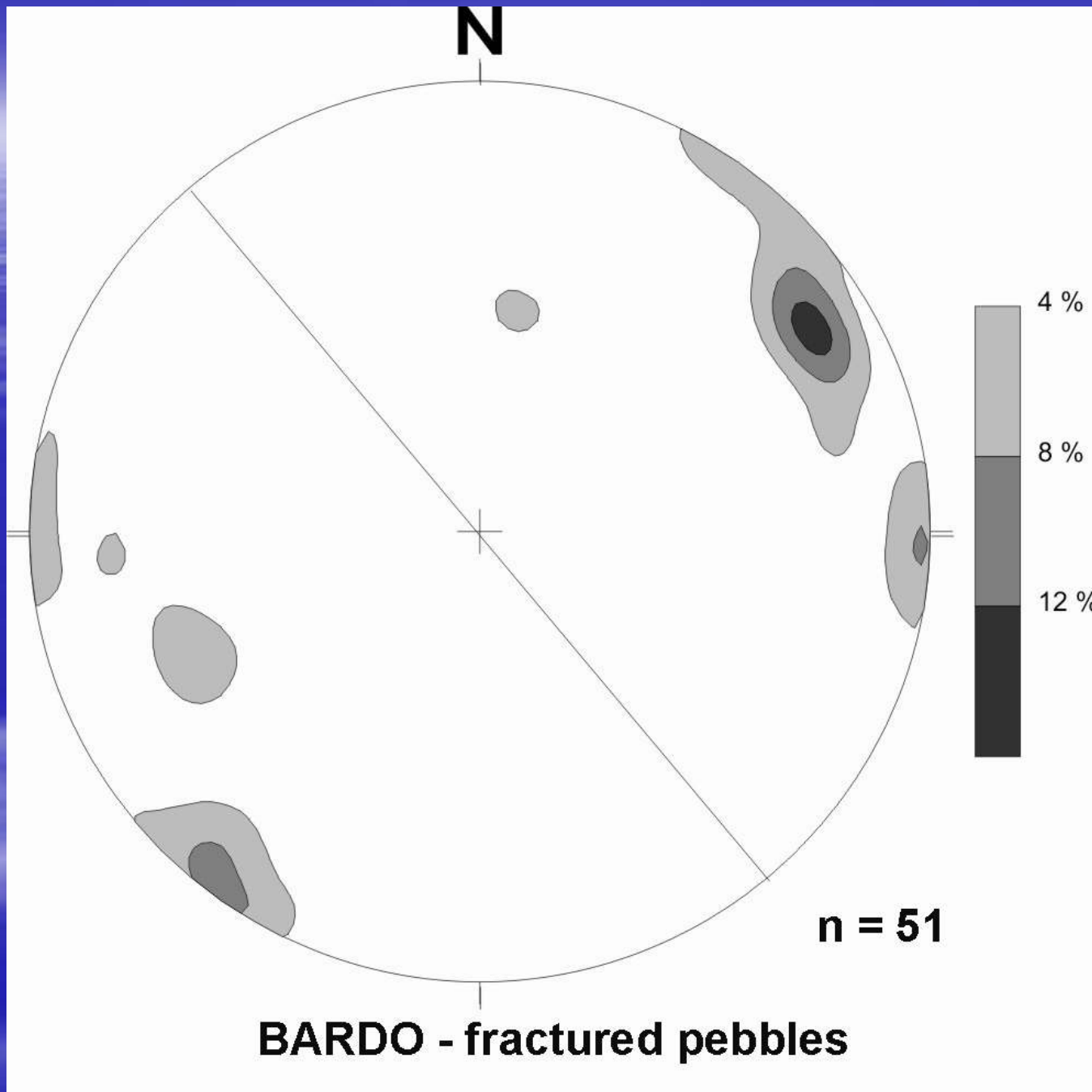
Faults active in the Tertiary and Quaternary: 1 – faults with undetermined sense of throw; 2 – faults with confirmed sense of throw: uBK – Karkonosze Marginal Fault, uR – Rębiszów Fault, uJ – Jerzmanowa Fault, rR-M – Roztoki-Mokrzyszów Graben, uStrz – Strzelin Fault, uBG – Biała Glucholaska Fault, rP-K – Paczków-Kędzierzyn Graben; 3 – new geodynamic profiles; 4 – geodynamic network points; 5 – isolines of recent vertical crustal movements according to WYRZYKOWSKI (1985); 6 – geodynamic polygons: A – “Śnieżnik Massif”, B – “Paczków Graben”, C – “Stołowe Mts.”; 7 – national border

Cacoń & Dyjor 2002



Recent vertical crustal movements in the Paczków Graben (based on Cacoń & Dyjor, 1995)

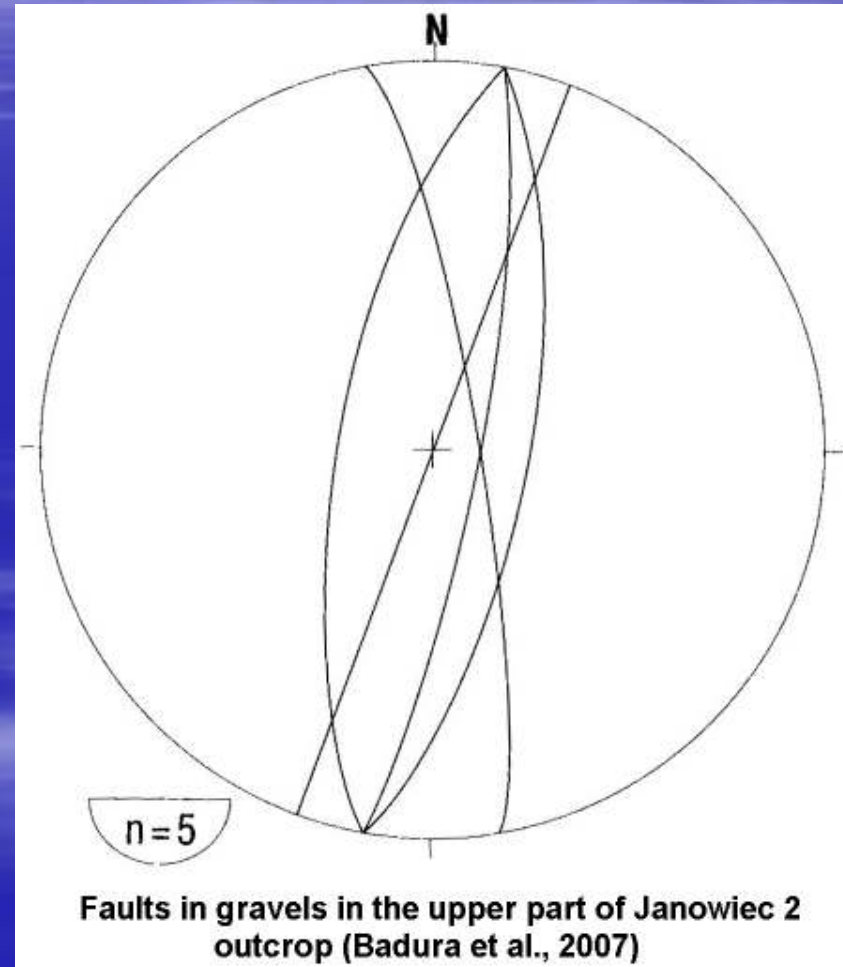




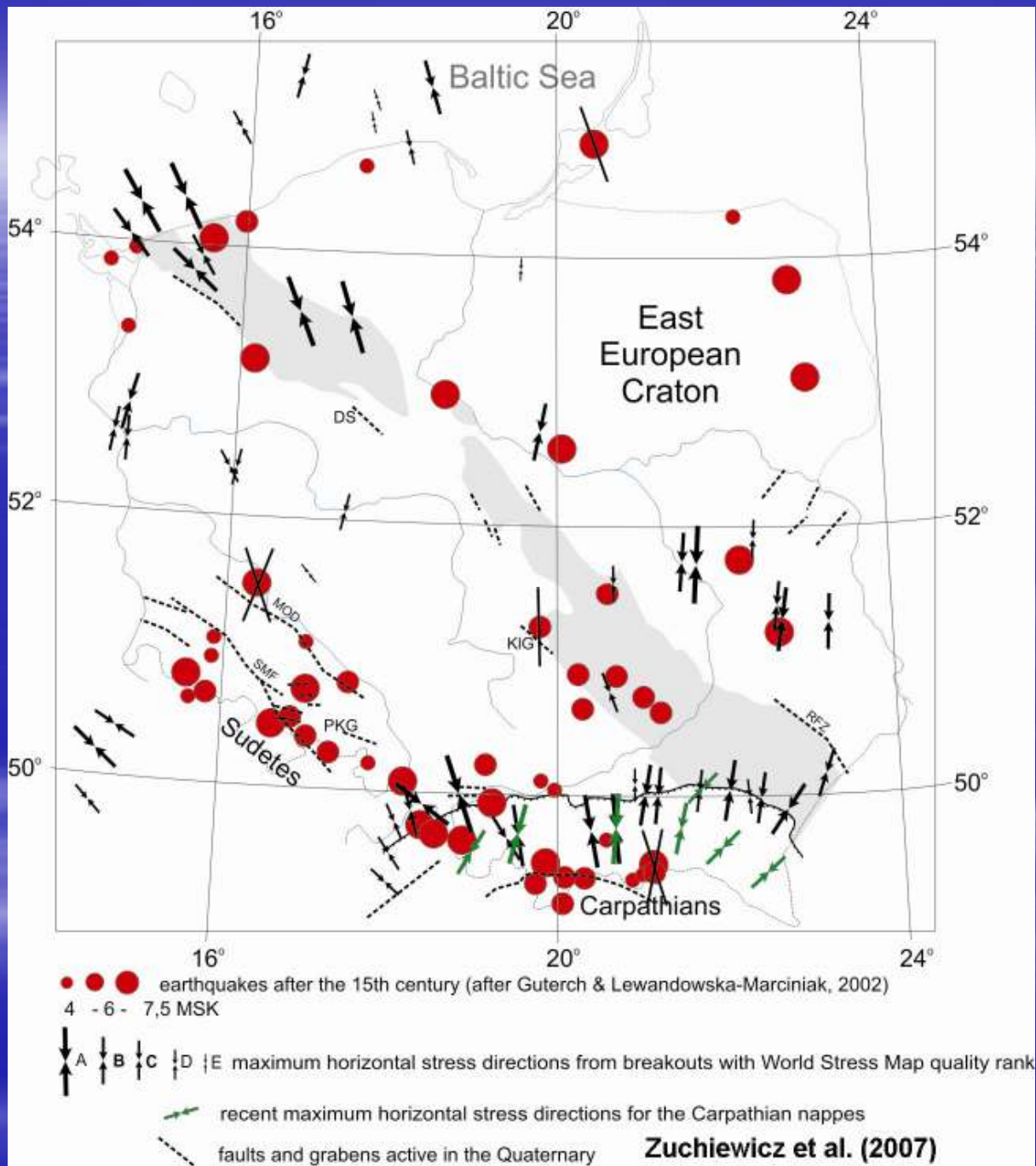
SMALL-SCALE FAULTS

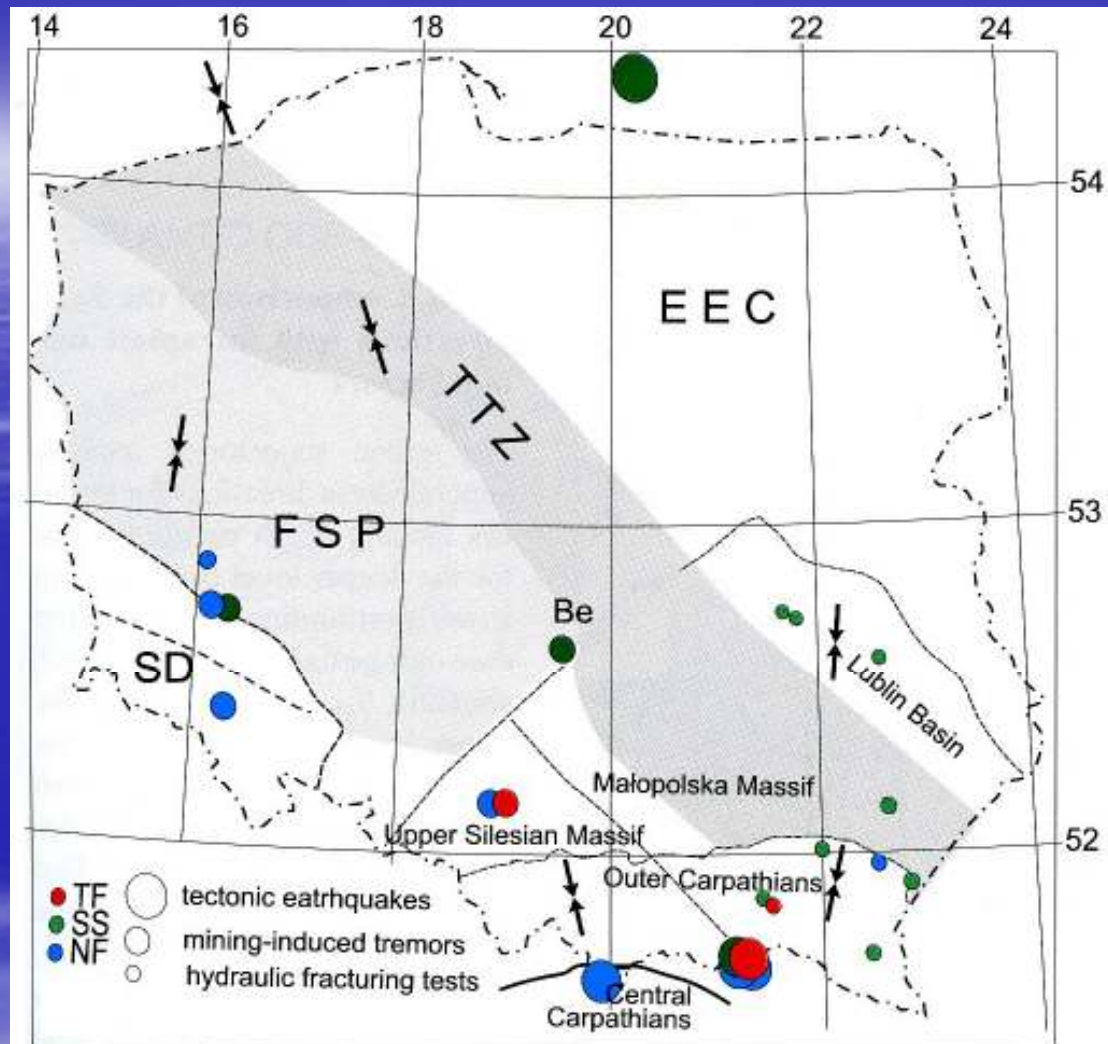


Small-scale faults in the upper (A) part of Janowiec 2 outcrop (Badura et al., 2007)



Faults in gravels in the upper part of Janowiec 2 outcrop (Badura et al., 2007)

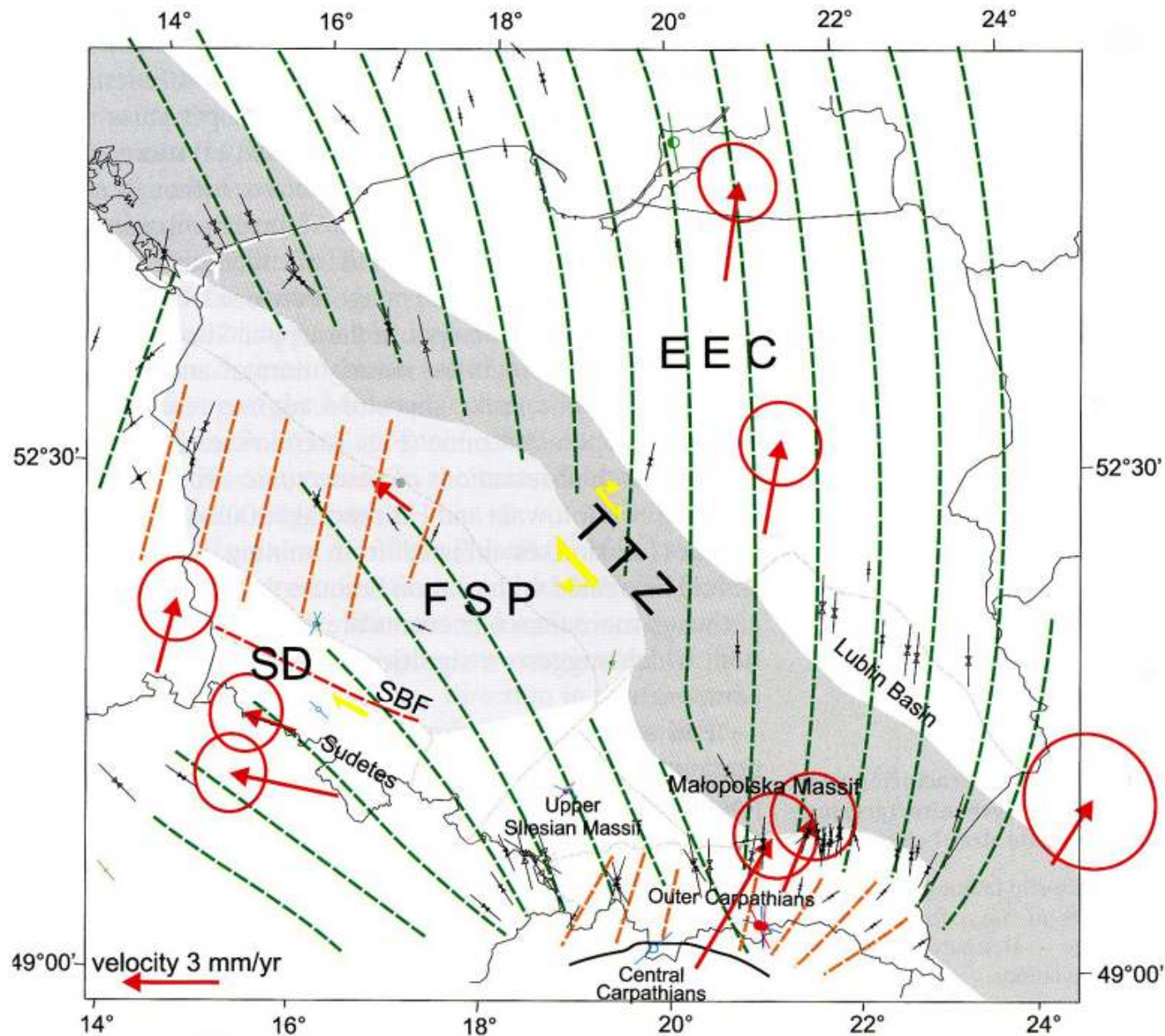




Jarosiński 2006

Distribution of stress regime data from hydro-fracturing tests (small circles) and from natural earthquake focal mechanism (greatest circles) and mining-induced tremors (intermediate size of circles)

Stress regimes: TF - thrust faulting, SS - strike-slip faulting, NF - normal faulting; arrows indicate mean direction of SHmax; Be - Belchatów mine



Comparison of the S_{Hmax} directions with intraplate motion vectors

The green trajectories indicate general stress directions for the areas lacking stress partitioning or for the deeper level in the case of stress partitioning. In the latter case orange trajectories are added, showing S_{Hmax} directions for the upper level. For comparison the World Stress Map data are shown in the background

Red arrows show directions of the intraplate motions (after Hetty, 1998); length of each arrow is proportional to the velocity; one-sigma error ellipse is attached to each arrow. Yellow arrows show hypothetical strike-slip motions along the TTN and the Sudetic Boundary Fault (SBF) that might be responsible for discrepancy between directions of S_{Hmax} and the intraplate motions.

after Jarosiński (2006)

CONCLUSIONS

Analysis of faceted spurs and morphometric parameters of small catchment areas on the Sudetic Marginal Fault points to moderate tectonic activity of the SMF footwall and allows us to conclude about Pliocene-Quaternary uplift, particularly important in the Rychlebské (Złote) and Sowie Mts. segments. Uplift of the last area most probably followed rapid cooling around 7-5 Ma, as shown by apatite fission-track studies of Aramowicz *et al.* (2006).

These observations appear to support earlier views on the normal character of faulting along the SMF, confirmed as well by some results of repeated GPS campaigns.

It is worth to note, however, that recent studies of fractured pebbles in Late Pleistocene fluvial gravels in the Bardo Mts. segment of the SMF indicate a dextral component of motion. Right-lateral reactivation of the SMF is also pointed out by GPS data (*cf.* Hefty, 1998) and finite element modelling of recent stresses in Europe (*cf.* Jarosiński, 2006).